*Geol. Mag.* **149** (*6*), *2012, pp. 945–963. © Cambridge University Press 2012*
doi:10.1017/S0016756812000040


# New insights into the polyphase evolution of the Variscan suture zone: evidence from the Staré Město Belt, NE Bohemian Massif

MIROSŁAW JASTRZĘBSKI*

Institute of Geological Sciences, Polish Academy of Sciences, Research Centre in Wrocław, Podwale St. 75, PL-50449 Wrocław, Poland

(*Received* 6 May 2011; *accepted* 5 January 2012; *first published online* 28 February 2012)

**Abstract** – Forming a northern continuation of the Moldanubian Thrust Zone, the Staré Město Belt comprises an E-verging thrust stack of three narrow lithotectonic units that exhibit variations in their respective *P–T* records. The upper and lower units form the respective margins of the hanging wall and footwall of the suture zone and are dominated by amphibolite grade metasedimentary successions. The middle unit is defined by an elongated body of MORB-like amphibolites that contains inserts of migmatized mica schists. Integrating both structural studies and pseudosection modelling in the MnNCKFMASH system shows that the present-day tectonic architecture of the Staré Město Belt is the result of a polyphase Variscan evolution. During a frontal, WNW–ESE-directed (in present-day coordinates) collision between the Bohemian Massif terranes and the Brunovistulian terrane, the metasedimentary rocks of the Staré Město Belt experienced tectonic burial to depths corresponding to 7–9 kbar. The continuous indentation and underthrusting of the Brunovistulian terrane led to top-to-the-ESE folding and uplift of these rocks to depths corresponding to 5.5–6.0 kbar at peak temperature. At depths corresponding to 5.5 kbar, the Staré Město Belt underwent subsequent dextral (top-to-the-NNE) shearing that was locally associated with nearly isobaric heating, possibly related to the emplacement of a Carboniferous tonalite body in the axial part of the Staré Město Belt. Subsequent tectonic compression resulted in the Variscan WNW-dipping metamorphic foliations becoming locally (N)NE- or ESE-dipping.

Keywords: Bohemian Massif, Moldanubian Thrust Zone, Staré Město Belt, *P–T* pseudosection thermobarometry, Variscan suture zone, polyphase structural evolution.

## 1. Introduction

The Variscan orogenic belt is the result of a Late Palaeozoic accretion of several terranes belonging to the Armorican Terrane Assemblage and the 'Old Red' continent (e.g. Tait *et al*. 1997; von Raumer, Stampfli & Bussy, 2003) (Fig. 1a). Understanding the tectonometamorphic evolution of the boundary zones between these terranes is of primary importance for the tectonic reconstruction of the European Variscides. A westerly-dipping Moldanubian Thrust Zone forms the boundary between the Bohemian Massif terranes and the Brunovistulian terrane (Fig. 1b). The nature of the Moldanubian Thrust Zone is, however, much debated: it could be a frontal collision zone that contains ocean crust remnants, or it could be a late Variscan intracontinental transpression zone (see review in Finger *et al*. 2007). In the Sudetes Mountains of the NE Bohemian Massif, the Moldanubian Thrust Zone is expressed as the narrow tectonic zone known locally as the Staré Město Belt. This belt may be a suture zone, a proposition supported by the presence of an extended body of Early Palaeozoic mid-ocean ridge basalt (MORB)-like amphibolites situated in its axial part (e.g. Poubová & Sokol, 1992; Floyd *et al*. 1996) and the occurrence of high-pressure rocks that are associated with subduction of the Brunovistulian terrane (Štípská, Pitra & Powel, 2006). In addition, the adjacent Saxothuringian/Moldanubian-derived and Brunovistulian-derived tectonic units show very different protolith ages (e.g. Kröner *et al*. 2000) and different inherited zircon components (e.g. Friedl *et al*. 2000; Żelaźniewicz *et al*. 2005; Jastrzębski *et al*. 2010).

The Staré Město Belt is, therefore, of regional importance and its precise role in the Variscan orogeny needs to be understood. But interpreting the metamorphic fabrics within the Staré Město Belt, as well as its hinterland and foreland units, has proven problematic. It does seem clear that the tectonic development of the Staré Město Belt was dominated by Carboniferous dextral (top-to-the-NNE) transpression and the syn-tectonic emplacement of a major tonalitic sill (Parry *et al*. 1997; Štípská *et al*. 2001; Štípská, Schulmann & Kröner, 2004). However, tectonometamorphic events that pre-date this Carboniferous tonalite intrusion are revealed by the occurrence of pre-tonalite, early deformational structures observable in metamorphic xenoliths (Parry *et al*. 1997). There is also evidence of a Cambro-Ordovician metamorphic event that might have affected the Variscan evolution of the region (e.g. Štípská *et al*. 2001; Štípská, Schulmann & Kröner, 2004; Lexa *et al*. 2005). Moreover, in contrast to the dextral movements affecting the belt's axial lithologies, syn-metamorphic

* Email: mjast@interia.pl

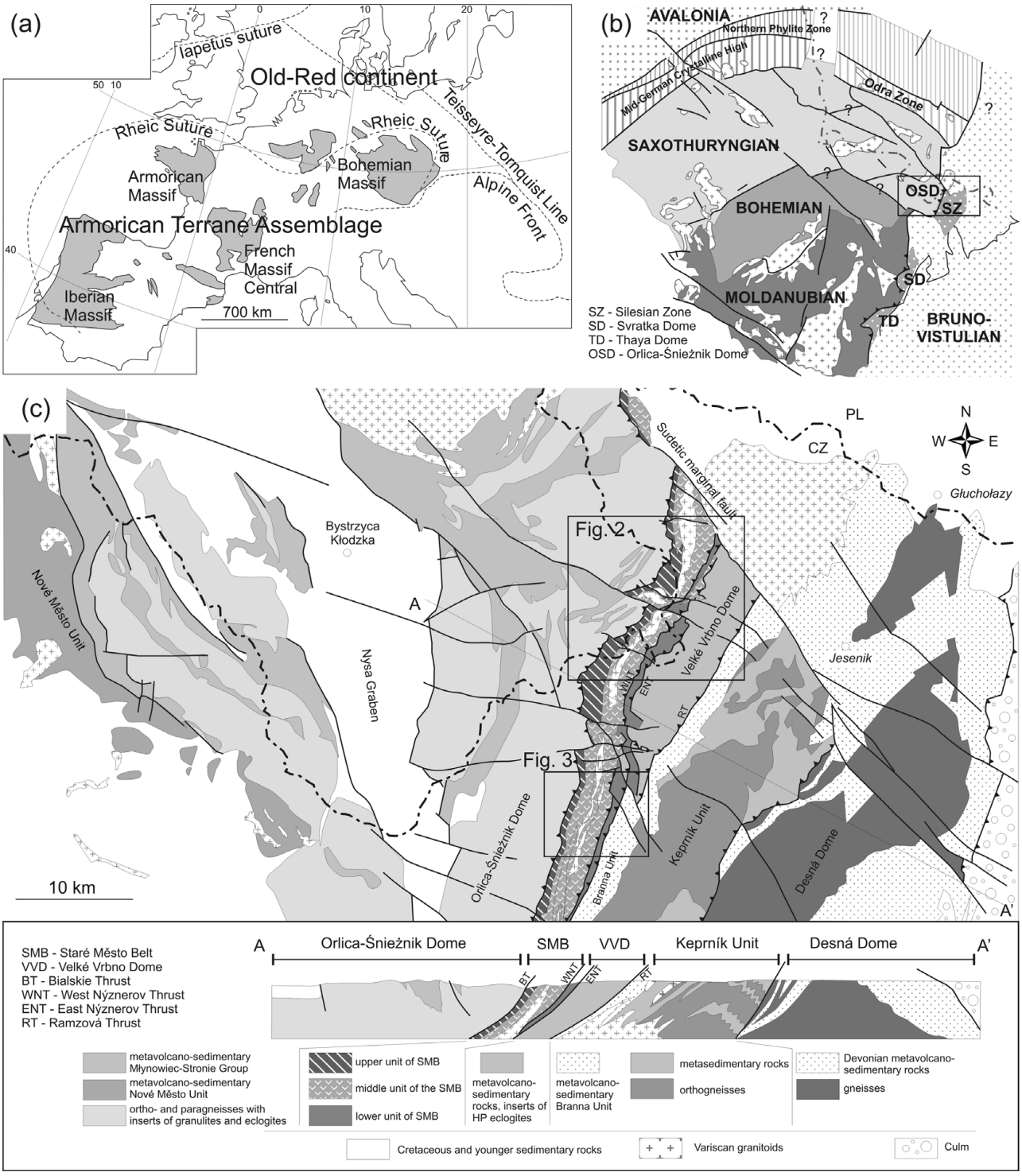


Figure 1. (a) The Variscan massifs and main tectonic boundaries in central Europe (modified after Linnemann *et al*. 2008). (b) Bohemian Massif with adjacent terranes (modified after Franke & Żelaźniewicz, 2002). (c) Geological map and cross-section through the boundary between the Orlica–Śnieżnik Dome and the Moravosilesian domain (compiled from Don, 1982; Sawicki, 1995; Schulmann & Gayer, 2000).

tectonic transport in an E–W direction has been postulated for the hinterland (e.g. Don *et al*. 1990; Jastrzębski, 2009) and the foreland of the collisional zone (e.g. Cháb *et al*. 1994; Żelaźniewicz *et al*. 2005).

This paper examines the mesostructures, microstructures and mineral compositions of the metasedimentary rocks of the Staré Město Belt, with the aim of clarifying several key interpretative elements: the pressure–temperature–deformation histories of these metasediments and the nature of the lithological contacts within the belt; the tectonometamorphism within and across the boundary between the Saxothuringian/Moldanubian and Brunovistulian terranes; and the possible existence of Cambro-Ordovician metamorphic fabrics in the metasedimentary rocks. The data in this paper are

https://doi.org/10.1017/S0016756812000040 Published online by Cambridge University Press

discussed in terms of the position of the three lithotectonic units that comprise the Staré Město Belt and the implications this has for the structural context of the Variscan orogen itself, not least whether the Staré Město Belt can be thought of as a Variscan suture zone.

## 2. Geological setting

### 2.a. Geology of the NE part of the Bohemian Massif

The Moldanubian Thrust Zone represents a 300 km long Variscan front stretching from northeastern Austria through the Moravian Region in the Czech Republic to the Sudetes Mountains in SW Poland (Fig. 1b). In its southern part, the Moldanubian Thrust divides the Armorica-derived Moldanubian terrane from the Neoproterozoic gneisses and overlying metasedimentary rocks of the Thaya and Svratka domes that form the westernmost part the composite Brunovistulian terrane (e.g. Finger *et al*. 2000; Żelaźniewicz *et al*. 2009). The northern continuation of the Moldanubian Thrust Zone is the Staré Město Belt. This belt is ∼55 km long, trends NNE–SSW, and forms a narrow tectonic zone that separates the Orlica–Śnieżnik Dome in the hinterland from the Silesian domain (Velké Vrbno Dome, Keprník and Branna units, Desna Dome) in the foreland (Fig. 1c).

The Orlica–Śnieżnik Dome comprises medium-grade Early Palaeozoic gneisses and metasedimentary rocks of the Młynowiec-Stronie Group with intercalations of high-grade eclogites and granulites (e.g. Don, Skácel & Gotowała, 2003). Rocks of the Młynowiec-Stronie Group were involved in a Variscan continental collision that led to their burial and amphibolite-facies metamorphism (e.g. Jastrzębski, 2009; Skrzypek *et al*. 2011*b*) synchronous with an exhumation of the migmatized lower crustal orogenic root and its vertical extrusion in mid-crustal levels (e.g. Štípská, Schulmann & Kröner, 2004). Structural studies on rocks of the Orlica–Śnieżnik Dome have revealed the importance of syn-metamorphic E–W-directed shortening (e.g. Don *et al*. 1990) that presumably preceded the dextral and sinistral movements along a N(NW)–S(SE) direction (Murtezi, 2006; Jastrzębski, 2009).

Neoproterozoic and Devonian rocks of the Silesian domain represent an imbricated accretionary prism of the Brunovistulian terrane metamorphosed under medium-pressure conditions (Schulmann & Gayer, 2000). Some high-pressure eclogites are dispersed within the Velké Vrbno Dome, the westernmost unit of the Brunovistulian terrane, and record the underthrusting of the Neoproterozoic Brunovistulian terrane crust below the Bohemian Massif terranes (Štípská, Pitra & Powell, 2006). The extensional, W-vergent metamorphic fabrics (Cháb *et al*. 1994) can be correlated with the westward subduction and early stages of the tectonic burial (Żelaźniewicz *et al*. 2005). The younger E-vergent structures were presumably connected with an inversion of the regional shearing that was caused by the progressive collision between the Brunovistulian terrane and the Bohemian Massif terranes, giving a subsequent dextral transpressional component (Żelaźniewicz *et al*. 2005).

### 2.b. Tripartite structure of the Staré Město Belt

Geological mapping within the Staré Město Belt by Kasza (1964) and Don, Skácel & Gotowała (2003) revealed three narrow, NNE-stretched, W-dipping lithotectonic units: they are classified here as the upper, middle and lower unit, respectively (Figs 2, 3).

The upper, westernmost 1–3 km wide unit of the Staré Město Belt underthrusts the western gneisses of the Orlica–Śnieżnik Dome and is composed of mica schists of the 'Hranična Formation' and is interlayered with felsic metavolcanic rocks, graphitic quartzites, marbles and amphibolites (Skácel, 1989; Don, Skácel & Gotowała, 2003).

The middle unit occupies the axial part of the Staré Město Belt and consists mainly of MORB-like, Cambro-Ordovician amphibolites (Opletal *et al*. 1990; Poubová & Sokol, 1992; Floyd *et al*. 1996). Leptyno-amphibolites occur at the base, while metagabbros occur at the top (e.g. Štípská *et al*. 2001). These rocks are locally accompanied by migmatized paragneisses and mica schists as well as a ∼340 Ma, ∼1 km wide, tonalite sill (Parry *et al*. 1997, Štípská, Schulmann & Kröner, 2004). The leptyno-amphibolites of the middle unit are believed to have experienced a pre-Variscan high-temperature–medium-pressure event, presumably connected with a widespread Cambro-Ordovician extension event (Kröner *et al*. 2000; Štípská *et al*. 2001, 2004; Lexa *et al*. 2005). The presumed Cambro-Ordovician metamorphism was probably similar to (Lexa *et al*. 2005) or slightly higher grade than the Variscan one (Parry *et al*. 1997), lying in the range 7–9 kbar and 800–900 °C. The Early Palaeozoic metamorphic episode was originally suggested by the presence of ∼500 Ma old zircons in melt patches that cross-cut the main fabric of the leptyno-amphibolites (Kröner *et al*. 2000). This event is thought to have made the middle unit rheologically stiff during the Variscan orogeny (Štípská, Schulmann & Kröner, 2004).

The lower, easternmost, 1–2 km wide lithotectonic unit of the Staré Město Belt is located between the East and West Nýznerov thrusts and is mainly composed of metapelites and paragneisses (the so-termed 'Skorošice series') with intercalations of amphibolites (metagabbros), eclogites and serpentinites (Don, Skácel & Gotowała, 2003). However, rocks assigned by Don, Skácel & Gotowała (2003) to the lower unit of the Staré Město Belt (Fig. 2) may, in fact, belong to the Velké Vrbno Dome, and thus to 'the Micaschist Zone', which is the uppermost part of the Brunovistulian terrane (Štípská, Pitra & Powell, 2006).

## 3. New structural data

The metasedimentary rocks of the Staré Město Belt have undergone a complex structural and metamorphic

https://doi.org/10.1017/S0016756812000040 Published online by Cambridge University Press

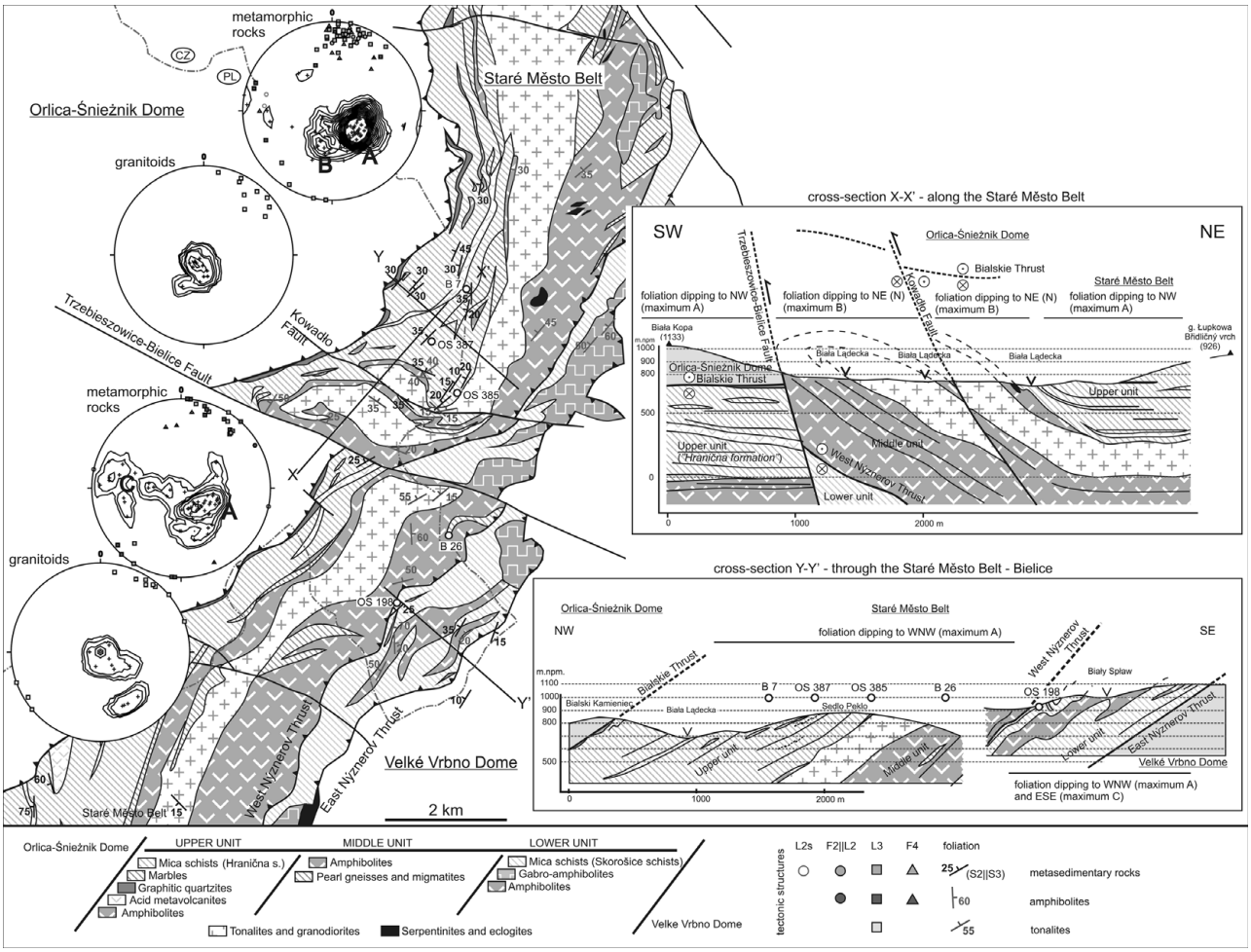


Figure 2. Geological cross-sections and stereograms showing orientation of tectonic structures in the northern part of the Staré Město Belt. Lines X–X′ and Y–Y′ correspond to cross-section locations. New structural data are drawn on the base map of Don, Skácel & Gotowała (2003).

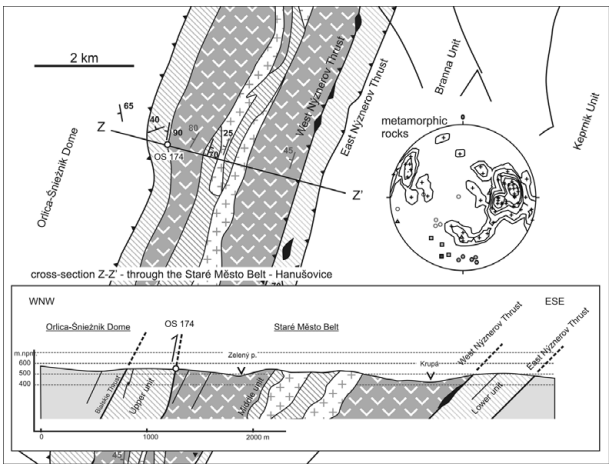


Figure 3. Geological cross-section and orientation of the tectonic structures in the southern part of the Staré Město Belt. New structural data are drawn on the base map of Don, Skácel & Gotowała (2003).

development (Fig. 4) that led to the formation of small-scale leucosome bodies. These range from ovoid patches a few centimetres in diameter to distinct, 20 cm thick, veins subparallel to a local foliation (Fig. 5).

The dominant penetrative S2 schistosity is axial planar to tight or isoclinal, E-verging, mesoscopic F2 folds (Fig. 4a). Relics of an older, S1 foliation are better preserved in the felsic metavolcanic rocks than in the adjacent less rigid mica schists, where the S1 planes were preserved in the form of inclusion trails in garnet porphyroblasts (Fig. 6a, b). The inclusion trails can be either straight in the garnet cores and sigmoidally curved within the garnet rim, or curved from core to rim: this latter indicates continuous garnet growth during the D2 deformation. An intersection of S1 and S2 has produced the L2 intersection lineation, which, together with the F2 fold axes, plunges shallowly towards the N(NNE) in the north of the Staré Město Belt (Fig. 2), and towards the S in the south of the study area (Fig. 3). The S2 planes were zonally reactivated to form an S3 foliation and the development of an associated L3 stretching mineral lineation, the result of top-to-the-NNE(N, NE) (dextral) ductile shearing (Fig. 4b). The leucosome patches that are sporadically observed in the upper unit and regularly observed in the middle and lower units sometimes superimpose the

https://doi.org/10.1017/S0016756812000040 Published online by Cambridge University Press

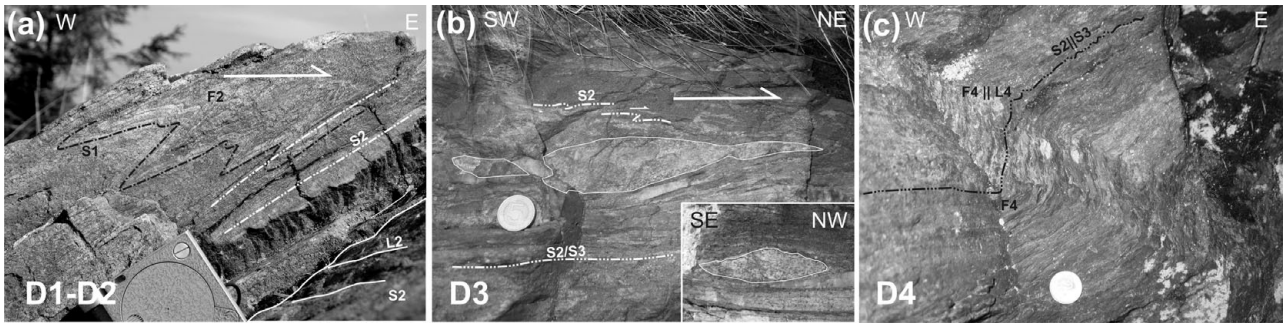


Figure 4. Field photographs showing small-scale meso-structures developed in Staré Město Belt metasediments. (a) E-vergent tight F2 folds developed in felsic metavolcanic rocks. (b) Sigma-shaped granitic segregation and asymmetric folds in adjacent metasediments, showing top-to-the-NNE sense of shear. (c) N–S-trending open F4 folds and parallel L4 crenulation lineation developed in mica schists of the upper unit. Coin diameter is 25 mm.

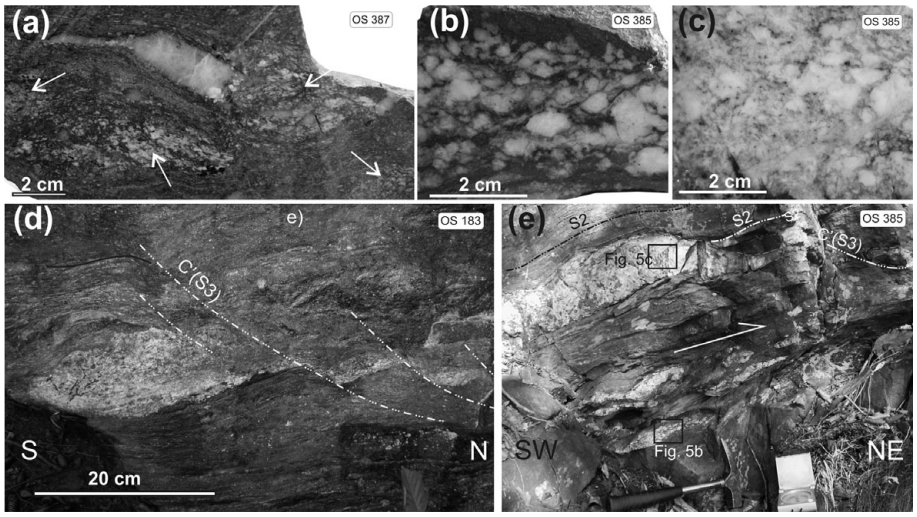


Figure 5. Field photographs showing evidence of late-D2 formation of leucosome patches and veins. (a) Garnet-bearing mica schists with leucosome patches indicated by arrows; upper unit. (b) and (c) Vein material representing a mixture of melt and relict precursor metamorphic rock. (d) Leucocratic melt pods within mica schists of the lower unit. (e) Leucocratic veins subparallel to the S2 fabric in amphibolites intercalated by mica schists; upper unit.

S2 foliation and/or are deformed by the S3 shear zones, which indicates that the localized partial melting and development of granitic segregations represent a pre-D3 deformation event (Fig. 4b, 5).

The composite S2‖S3 foliation is generally parallel to the Staré Město Belt tectonic boundaries and has moderate to steep W(NW) dip (maximum A in Fig. 2). Locally, the strike of the foliation changes to N or NE and the dip changes to shallow/moderate: both trends suggest a subsequent rotation (maximum B in Fig. 2). Locally, the S2 foliation dips to the ESE (maximum C) (Fig. 2), also suggesting a subsequent rotation. The last generation of mesostructures links to E–W-directed shortening that took place under semi-brittle deformation conditions. This tectonic stage gave rise to open, concentric or kink N–S-trending mesofolds ranging in amplitude from several decimetres down to microcrenulations. The F4 folds are doubly vergent both E- and W-ward, their axial planes often forming complementary surfaces. In contrast to the F2 folds, they lack an axial planar foliation (Fig. 4c).

## 4. Petrography, mineral chemistry and *P–T* evolution

### 4.a. Methods of investigation

Pressure–temperature–deformation relationships were studied in the metasedimentary and felsic metavolcanic rocks in the three lithotectonic units of the Staré Město Belt. Three samples of metasedimentary rocks, one from each unit, were selected for detailed petrological study. The samples were selected on the basis of their location along a single transect through the northern, best-exposed part of the Staré Město Belt (Fig. 2), in addition to their mineral compositions and well-defined structural–metamorphic relationships. The pseudosection and isopleth calculations were undertaken in the system $MnO–Na_2O–CaO–K_2O–FeO–MgO–Al_2O_3–SiO_2–H_2O$ (MnNCKFMASH), which is thought to be close to the real bulk chemical system of the studied samples. Effective bulk compositions were obtained using thin-sections via a combination of optical imaging and back-scattered electron imaging, from which modal proportions of each phase could be

https://doi.org/10.1017/S0016756812000040 Published online by Cambridge University Press

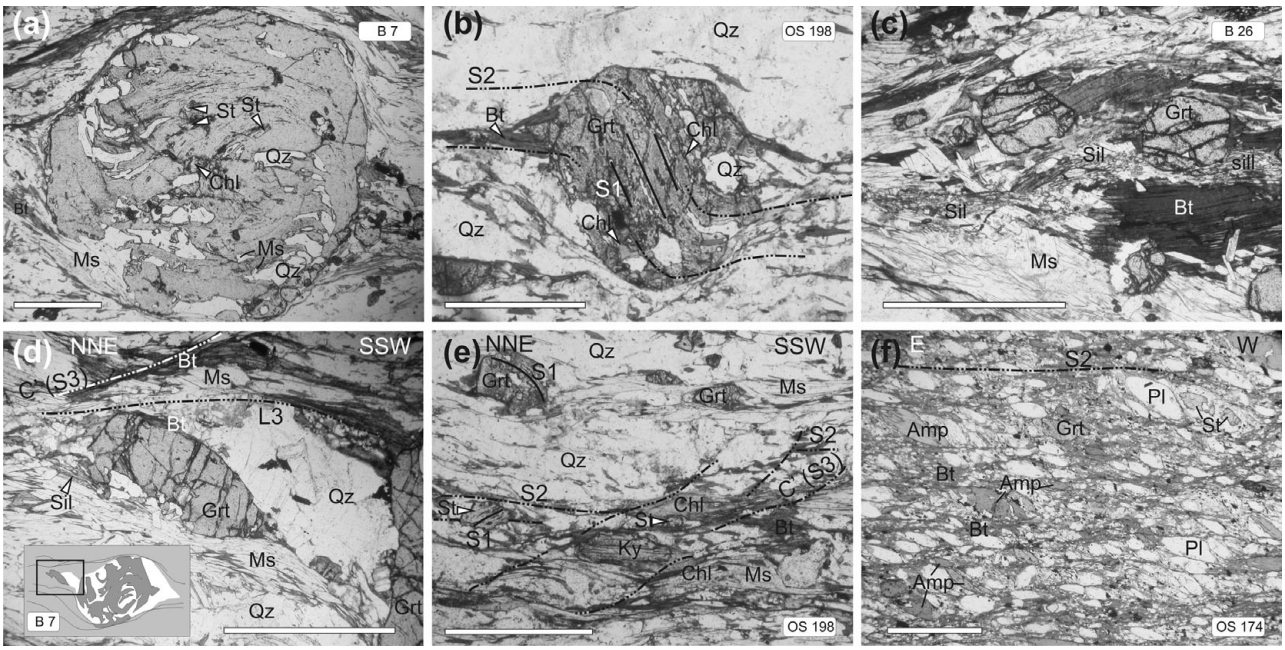


Figure 6. Plane polarized light photomicrographs showing relationships between metamorphic fabrics and successive tectonic stages. (a) Spirally arranged inclusions of St–Chl–Ms–Qz in garnet porphyroblast. Mica schists of the upper unit. (b) S1–S2 microstructural relationships in mica schist of the lower unit. (c) High-temperature fabric composed of Grt–Bt–Ms–Sil assemblage in mica schists of the middle unit. (d) Sil–Ms–Grt–Qz assemblage forming top-to-the-NNE asymmetric pressure shadow around a large garnet porphyroclast. Mica schist of the upper unit. (e) The S2 foliation cut by C′ planes in mica schist of the lower unit. (f) Mylonite developed along the boundary between the upper and middle units. Scale bar is 1 mm.

calculated. Average compositions for each phase were determined using chemical analyses; modal proportions of almandine, grossular, spessartine and pyrope in garnet grains were obtained using detailed compositional profiles. This method of calculation of bulk composition allows for an accurate estimation of bulk compositional changes in the coarser garnets due to elemental fractionation during growth (Dutch, Hand & Kelsey, 2010). Major element compositions, which formed the basis of the phase equilibria modelling, were analysed using the Cameca SX100 Electron Microprobe at the Electron Microprobe Laboratory of the Inter-Institute Analytical Complex for Minerals and Synthetic Substances at the University of Warsaw. Additionally, a garnet profile from sample OS198 was obtained using a JEOL JSM 840A Electron Microprobe combined with a ThermoNoran system at the Institute of Geological Sciences of the Polish Academy of Sciences in Warsaw. The pressure–temperature (*P–T*) pseudosections were calculated using THERMOCALC software – incorporating the internally consistent thermodynamic data set of Holland & Powell (1998, dataset 55; November 2003 update) – and the activity–composition models of White, Pomroy & Powell (2005) for garnet and biotite, White, Powell & Holland (2007) for silicate melt, a combination of Mahar *et al*. (1997) and Holland & Powell (1998) for staurolite, Holland & Powell (2003) for plagioclase, Holland, Baker & Powell (1998) for chlorite, Coggon & Holland (2002) for muscovite, and Tinkham & Ghent (2005) for paragonite.

The mineral abbreviations used in this paper follow the recommendations of the IUGS (Whitney & Evans, 2010, as based on Siivola & Schmid, 2007, as based on Kretz, 1983). The mineral and isopleth abbreviations are as follows: Alm – almandine; Amp – amphibole; And – andalusite; Bt – biotite; Chl – chlorite; Cld – chloritoid; Grs – grossular; Grt – garnet; Ilm – ilmenite; Ky – kyanite; Mnz – monazite; Ms – muscovite; Pg – paragonite; Pl – plagioclase; Prp – pyrope; Qz – quartz; Rt – rutile; Sil – sillimanite; Sps – spessartine; St – staurolite; Tur – tourmaline; Zrn – zircon, and $X_{Alm}$: Fe/(Fe + Mn + Mg + Ca) × 100; $X_{Sps}$: Mn/(Fe + Mn + Mg + Ca) × 100; $X_{Prp}$: Mg/(Fe + Mn + Mg + Ca) × 100; $X_{Grs}$: Ca/(Fe + Mn + Mg + Ca) × 100; $X_{Fe}$ (Grt, St, Bt, Chl): Fe/(Fe + Mg) × 100; $X_{Ca}$ (Pl, Pg): Ca/(Na + K + Ca) × 100. The arrow sign '→' is here used to indicate a trend in mineral assemblage changes or compositional zoning.

### 4.b. Upper unit: Sample B7

#### *4.b.1. Microstructures*

Sample B7 was taken from the upper unit ('Hranična Formation') and contains quartz, muscovite, biotite, garnet, plagioclase, rutile, chlorite, paragonite, staurolite, sillimanite and tourmaline. The internal S1 foliation in the garnet porphyroblasts is mainly defined by the parallel alignment of quartz laminae and inclusions of paragonite, chlorite, staurolite, muscovite and rutile. Garnets with curved inclusion trails are frequently overgrown by secondary garnet rims, which contain fewer

https://doi.org/10.1017/S0016756812000040 Published online by Cambridge University Press

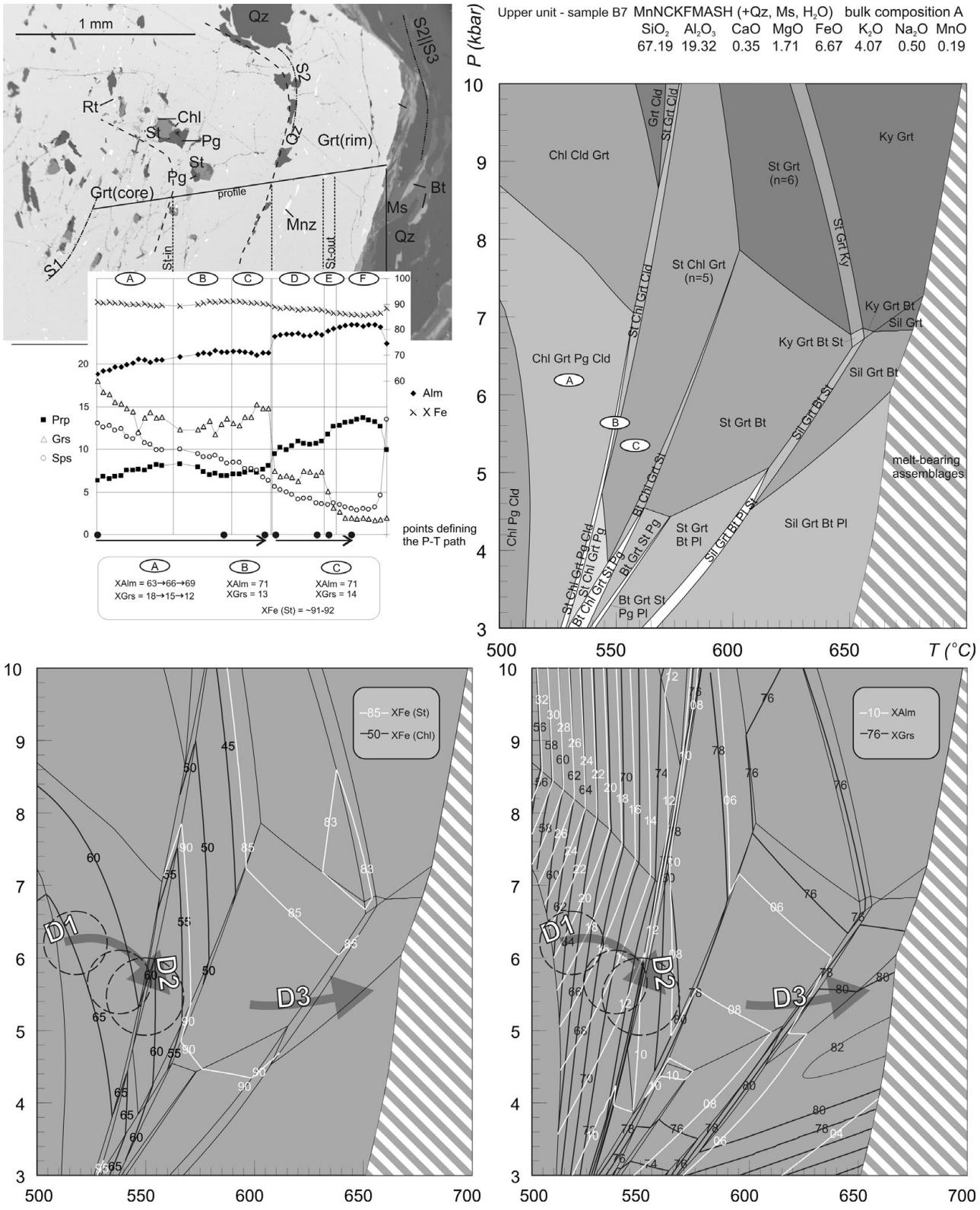


Figure 7. Mineral chemistry and thermobarometry for sample B7 of the upper unit. *P–T* pseudosection was calculated using bulk composition 'A' (see text). Lower diagrams show compositional isopleths for garnet, staurolite and chlorite. Dashed-line circles are derived from garnet compositional isopleths. Grey arrows indicate the *P–T* conditions of garnet growth. The arrow representing growth of the garnet rim is derived from calculations using bulk composition 'B' (see Fig. 8).

inclusions (Fig. 6a). These garnet rims contain quartz, but only rare inclusions of biotite and muscovite. The garnet profile across one of these porphyroblasts is presented in Figure 7. The matrix foliation S2‖S3 is defined by quartz, muscovite, biotite, plagioclase, tourmaline and sillimanite. Sillimanite was observed in N–S-oriented thin-sections where its occurrence is restricted to asymmetric pressure shadows around

https://doi.org/10.1017/S0016756812000040 Published online by Cambridge University Press

Table 1. Representative analyses of minerals in Staré Město Belt upper unit sample B7

| Mineral<br>Position | Grt<br>core, zone A | Grt<br>rim, zone F | Chl<br>inclusion | St<br>inclusion | Bt<br>matrix, core | Bt<br>matrix, rim | Ms<br>matrix | | Pg<br>inclusion | Pl<br>matrix |
|---|---|---|---|---|---|---|---|---|---|---|
| Wt % oxide | | | | | | | | | | |
| $SiO_2$ | 36.98 | 37.05 | 22.62 | 27.55 | 34.87 | 33.40 | 46.01 | | 39.68 | 64.94 |
| $TiO_2$ | 0.14 | 0.01 | 0.04 | 0.58 | 2.02 | 2.18 | 0.72 | | 0.00 | n.a. |
| $Cr_2O_3$ | 0.00 | 0.02 | n.a. | 0.00 | n.a. | n.a. | n.a. | | n.a. | n.a. |
| $Al_2O_3$ | 20.88 | 21.14 | 24.49 | 55.65 | 19.60 | 18.67 | 36.10 | | 44.53 | 22.24 |
| $Fe_2O_3$ | 0.43 | 0.04 | n.a. | n.a. | n.a. | n.a. | n.a. | | n.a. | n.a. |
| FeO | 29.05 | 36.86 | 35.46 | 13.25 | 20.15 | 22.43 | 1.02 | | 0.62 | 0.00 |
| MnO | 5.91 | 1.62 | 0.91 | 0.57 | 0.25 | 0.30 | 0.00 | | 0.26 | n.a. |
| MgO | 1.62 | 3.12 | 6.62 | 0.73 | 7.42 | 7.52 | 0.66 | | 0.00 | 0.00 |
| CaO | 6.49 | 1.06 | 0.03 | n.a. | 0.10 | 0.27 | 0.00 | | 4.52 | 3.07 |
| $Na_2O$ | 0.02 | 0.00 | 0.01 | n.a. | 0.40 | 0.48 | 0.96 | | 4.86 | 10.21 |
| $K_2O$ | 0.00 | 0.00 | 0.00 | n.a. | 8.57 | 9.07 | 9.94 | | 0.11 | 0.10 |
| ZnO | n.a | n.a. | n.a. | 0.37 | n.a. | n.a. | n.a. | | n.a. | n.a. |
| Total | 101.52 | 100.92 | 90.18 | 98.70 | 93.38 | 94.32 | 95.41 | | 94.58 | 100.56 |
| No. of O | 12 | 12 | 28 | 23 | 22 | 22 | 22 | | 22 | 8 |
| Si | 2.953 | 2.973 | 4.912 | 3.787 | 5.421 | 5.254 | 6.097 | | 5.182 | 2.847 |
| Ti | 0.008 | 0.001 | 0.007 | 0.060 | 0.236 | 0.258 | 0.072 | | 0.000 | – |
| Cr | 0.000 | 0.001 | – | 0.000 | – | – | – | | – | – |
| Al | 1.966 | 1.999 | 6.268 | 9.019 | 3.591 | 3.461 | 5.638 | | 6.854 | 1.149 |
| $Fe^{3+}$ | 0.026 | 0.002 | 0.000 | – | 0.000 | 0.000 | 0.000 | | 0.000 | 0.000 |
| $Fe^{2+}$ | 1.940 | 2.474 | 6.440 | 1.523 | 2.620 | 2.951 | 0.113 | | 0.068 | 0.000 |
| Mn | 0.400 | 0.110 | 0.167 | 0.066 | 0.033 | 0.040 | 0.000 | | 0.029 | – |
| Mg | 0.193 | 0.373 | 2.143 | 0.150 | 1.720 | 1.764 | 0.130 | | 0.000 | 0.000 |
| Ca | 0.555 | 0.091 | 0.007 | – | 0.017 | 0.046 | 0.000 | | 0.633 | 0.144 |
| Na | 0.003 | 0.000 | 0.004 | – | 0.121 | 0.146 | 0.247 | | 1.231 | 0.868 |
| K | 0.000 | 0.000 | 0.000 | – | 1.700 | 1.820 | 1.680 | | 0.018 | 0.006 |
| Zn | – | – | – | 0.038 | – | 2.000 | – | | – | – |
| Total | 8.044 | 8.025 | 19.949 | 14.643 | 15.457 | 15.740 | 15.976 | | 14.015 | 5.015 |
| $X_{Fe}$ | 91 | 87 | 75 | 91 | 60 | 63 | 46 | $X_{Ca}$ | 33 | 14 |
| $X_{alm}$ | 63 | 81 | | | | | | | | |
| $X_{sps}$ | 13 | 4 | | | | | | | | |
| $X_{prp}$ | 6 | 12 | | | | | | | | |
| $X_{grs}$ | 18 | 3 | | | | | | | | |

n.a. – not analysed.

garnets, so defining the L3 lineation. Therefore, this sillimanite could be connected with the D3 stage of deformation (Fig. 6d).

#### *4.b.2. Parageneses and mineral chemistry*

With respect to mineral assemblage and garnet compositional changes, four mineral parageneses were identified that can be correlated with the separate parts of strongly zoned garnets. Garnet zones A, B and C represent an inclusion-rich garnet core, whereas garnet zones D, E and F represent an inclusion-poor, secondary garnet rim that is sometimes observed in the metapelites of the upper unit. Garnet core assemblages are composed of garnet, paragonite, chlorite, quartz, staurolite, rutile and ilmenite (Fig. 7). Towards the boundary of zone C, the chlorite–paragonite–quartz inclusions are curved, indicating continuous garnet growth at the start of the D2 deformation. Detailed microprobe analyses of garnet cores revealed a gradual, but tripartite, profile. The first part of this profile, zone A, is characterized by a gradual rimward increase in Fe and Mg ($X_{Alm}$ 63→69; $X_{Prp}$ 6→8) and a decrease in Mn and Ca ($X_{Sps}$ 16→12; $X_{Grs}$ 14→10). The second part of this profile, zone B, the middle part, is characterized by an increase in Fe and Ca (to $X_{Alm} = 72$; $X_{Grs} = 13$) and a decrease in Mg and Mn (to $X_{Prp} = 7$; $X_{Sps} = 9$). The third part of this profile, zone C, is characterized by an increase in Mg and Ca (to $X_{Prp} = 8$; $X_{Grs} = 14$) and a decrease in Fe and Mn (to $X_{Alm} = 71$; $X_{Sps} = 6$) (Fig. 7; Table 1). Staurolite inclusions in inclusion-rich garnet cores are ∼100 μm in diameter and homogeneous; however, $X_{Fe}$ content ranges from 91 to 93 in different grains. Paragonite inclusions are characterized by small phengitic and large margaritic substitutions ($X_{Ca} = 33$–37). Chlorite inclusions have $X_{Fe} = 75$.

The boundary between zones C and D is marked by distinctive quartz laminae and by discontinuity in the garnet zoning profile. This discontinuity is shown by a sharp increase in Fe and Mg and a decrease in Ca from ($X_{Prp} = 8$; $X_{Alm} = 71$; $X_{Grs} = 7$) to ($X_{Prp} = 9$; $X_{Alm} = 77$; $X_{Grs} = 5$). Zones E and F were distinguished by gradual changes in garnet composition within its rim, i.e. by a rimward increase in Fe and Mg ($X_{Alm}$ 80→82; $X_{Prp}$ 12→13) and a decrease in Ca and Mn ($X_{Grs}$ 5→2; $X_{Sps}$ 4→3). Matrix biotite is slightly zoned, with rimward increases in $X_{Fe}$ from 57 to 62.

#### *4.b.3. Pseudosection and isopleth modelling*

Owing to the presence of coarse-grained zoned garnet porphyroblasts that were possibly responsible for some fractionation of the bulk composition, two MnNCKFMASH pseudosections were calculated for sample B7. The first pseudosection is based on 'whole-rock' composition ('A') and gives information on the

https://doi.org/10.1017/S0016756812000040 Published online by Cambridge University Press

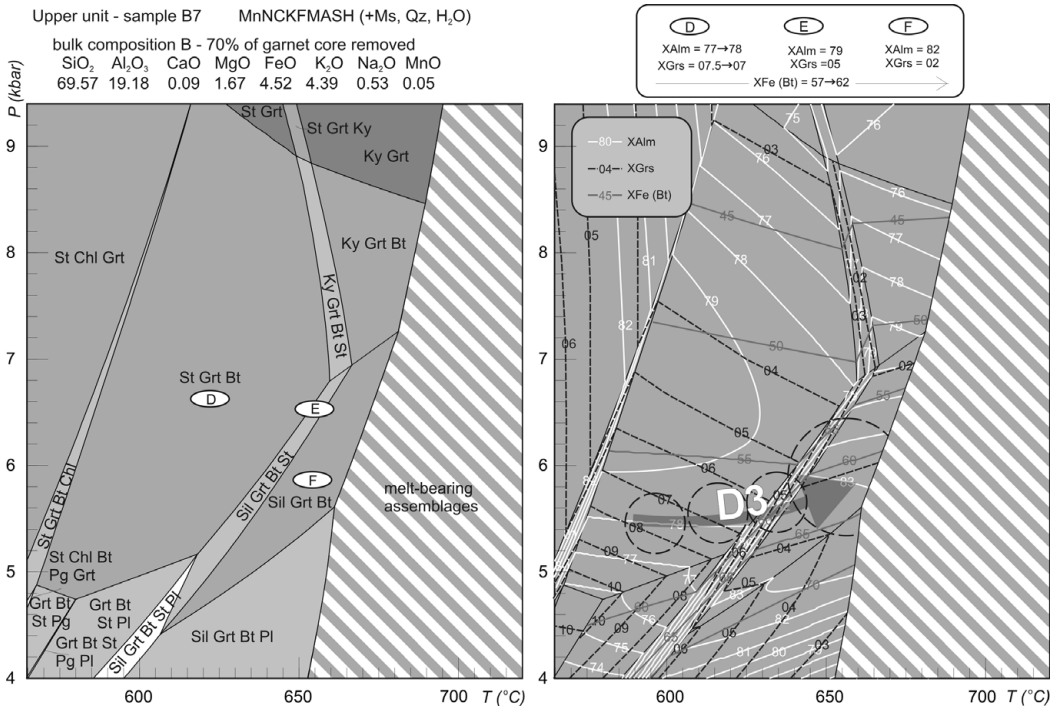


Figure 8. *P–T* pseudosection for sample B7 calculated using bulk composition 'B'. Right-side diagram shows selected compositional isopleths for garnet and biotite. Grey arrow indicates the *P–T* path for growth of the garnet rim.

stable mineral assemblage during growth of the garnet core (Fig. 7). Bulk composition 'B' represents the whole-rock composition with ~ 70 % of the garnet core composition removed from the assemblage and was used for modelling the stability of mineral assemblages that coexist with the garnet rim (Fig. 8). Subsolidus equilibria were calculated in detail for both types of bulk composition, with water assumed to be in excess. To constrain the stability field of staurolite-bearing assemblages, the stability of chlorite-, chloritoid- and $Al_2SiO_5$-assemblages were accounted for in the calculations. And because metapelite partial melting occurs adjacent to sample B7, melt-bearing assemblages were also calculated. The calculated pseudosections reveal a predominance of four- and five-variant fields and the presence of some six-variant fields at higher pressures and tri-variant fields at lower pressures.

The pseudosection and isopleth thermobarometry indicates that a staurolite-bearing mineral assemblage recognized in garnet cores (Fig. 7) presumably represents a narrow tri-variant field of Chl–Cld–St–Pg–Grt–Ms–Qz (zone B). The modelled compositional isopleths of the garnet and staurolite, representing the measured mineral compositions, are consistent with the stability fields of these mineral assemblages, with the exception of chlorite ($X_{Fe} = 75$). Such composition does not tie in with possible chlorite compositions within the garnet stability field; therefore, some of the chlorite inclusions probably represent an earlier, pre-garnet and lower-temperature mineral assemblage. The measured garnet compositions in zone A indicate that the pre-staurolite garnet core was in equilibrium with chloritoid; the latter could have been consumed during progressive metamorphic reactions. Contouring zone A for $X_{Alm}$, $X_{Sps}$ and $X_{Grs}$ and comparing the result with $X_{Fe}$ contours for staurolite indicates a rimward decrease of pressure from ~ 6.5 to 6.0 kbar associated with a slight temperature increase from ~ 520 to 550 °C in the inner part of zone A. Compositional changes observed within garnet cores (zones A, B and C) could be the result of change in mineral assemblages, i.e. the growth of staurolite at the expense of chloritoid and simultaneous disappearance of paragonite. These changes indicate that garnet grew continuously with the presence of staurolite during continuous pressure decrease (5.5 kbar at ~ 570 °C). But the decompression event is not entirely recorded by the garnet. The occurrence of kyanite along the S2 foliation in adjacent samples suggests that the estimated temperature of ~ 570 °C is the minimum temperature of the S2 foliation formation event.

Sharp compositional changes between garnet core and garnet rim (the boundary between zones C and D) indicate that garnet growth took place during two metamorphic episodes. The derived *P–T* trajectories indicate that the *P–T* path in between zones C and D is not recorded by the garnets. Compositional changes observed within garnet rims (zones D, E and F) could be the result of progressive change in mineral assemblages, i.e. the growth of sillimanite at the expense of staurolite. Narrower changes in garnet composition in the middle part of the garnet rim (zone E) suggest that the *P–T* path could cross the narrow four-variant field Sil–Grt–Bt–St–Ms–Qz. The specific mineral assemblage succession and the garnet and

https://doi.org/10.1017/S0016756812000040 Published online by Cambridge University Press

biotite isopleths suggest that the growth of the garnet rim, and that of the coexisting matrix phases, was controlled by a temperature increase from 600 to 650 °C under nearly isobaric conditions (5.5 kbar, see Fig. 8).

### 4.c. Middle unit: Sample B26

#### *4.c.1. Microstructures*

Sample B26 represents an intercalation of mica schist within the amphibolites from the axial part of the Staré Město Belt (Fig. 2). The origin of these metasediments within the middle unit is not clear. Evidence for interfingered contacts between the metasedimentary rocks and the body of the amphibolites (Fig. 2) may indicate their original relative positions. The mica schist contains quartz, muscovite, biotite, garnet, plagioclase, ilmenite, sillimanite, tourmaline, zircon and monazite (Table 2; Fig. 6c). In contrast to sample B7, garnets in the B26 sample are small, up to 0.5 mm in diameter, and scattered in the schistose matrix. In garnet cores, an internal S1 foliation is defined by a preferred orientation of biotite, muscovite and quartz inclusions. The matrix S2 foliation is mainly defined by the alignment of quartz and of biotite–muscovite–sillimanite laminae (Figs 6c, 9).

#### *4.c.2. Mineral chemistry, pseudosection and isopleth modelling*

Profiles of almandine, spessartine, pyrope and grossular in individual garnet grains remain flat from core to rim, suggesting post-growth cation diffusion (Table 2). Biotite composition is characterized by a progressive shift in $X_{Fe}$ values from 47 to 54 in biotite inclusions, to 61–62 in biotite flakes that define the matrix foliation. To constrain the stability fields of biotite-, garnet- and sillimanite-bearing assemblages, the stability of chlorite-, staurolite- and melt-bearing assemblages were accounted for in the calculations. Water and quartz were assumed to be in excess. The calculated MnNCKFMASH pseudosection is dominated by five- and six-variant fields with some four-variant fields at lower pressures. Pseudosection analysis indicates that the predominant mineral assemblage (A), represented by the six-variant field Grt(core)–Bt–Ms–Qz, is stable over wide *P–T* conditions (590–680 °C and 6–11 kbar). The mineral assemblage coexisting with the garnet rim (B), represented by the five-variant field Grt(rim)–Bt–Ms–Qz–Sil, is stable at 580–680 °C and 4–6 kbar. As the garnets of sample B26 were homogenized, possibly at high temperatures, their compositions cannot be reliably used to constrain a *P–T* path. Nevertheless, variations both in mineral parageneses and in biotite composition indicate a general trend of decompression (from ~ 10 kbar to 6 kbar) during garnet growth and the development of the matrix S2 foliation (Fig. 9). Temperatures of garnet growth are probably close to 680 °C, as the evidence of partial melting in K-feldspar-bearing mica schists was found in adjacent samples.

### 4.d. Lower unit: Sample OS198

#### *4.d.1. Microstructures*

Sample OS198 from the Skorošice mica schists (according to Don, Skácel & Gotowała, 2003) contains quartz, plagioclase, muscovite, biotite, garnet, chlorite, kyanite, staurolite and ilmenite. Quartz and plagioclase are the main mineral components. Garnet porphyroblasts (up to 2 mm) are dispersed in quartzo-feldspathic and mica-rich domains and form 8 % by volume. Garnet cores contain tabular plagioclase crystals, chlorite flakes, and lobate quartz and ilmenite inclusions. Parallel alignment of these minerals forms the S1 foliation. Muscovite and biotite occur both as small inclusions in garnet rims (associated with quartz and/or plagioclase) and as large flakes in the matrix. Preferred mineral alignments within garnet rims define a curved internal foliation that extends into the matrix S2 foliation (Fig. 6b). The matrix foliation is generally defined by compositional banding of wider quartzo-feldspathic domains and narrower mica-rich domains. The S2 foliation is reinforced by oblate quartz and plagioclase grains in the quartzo-feldspathic domains (Fig. 10) and by a parallel alignment of kyanite and staurolite. The staurolite contains an internal fabric similar to that observed in the garnets and which is defined by elongated quartz and ilmenite inclusions (Fig. 6e). Therefore, the garnet and staurolite probably have the same structural position despite staurolite not being observed as an inclusion in garnet. Chlorite often occurs along C′ planes that cross-cut the S2 foliation at an angle of ~ 30° (Fig. 6e). The orientation of the C′ planes suggests that they developed during the reactivation of the S2 foliation during the D3 tectonic stage.

#### *4.d.2. Parageneses and mineral chemistry*

Garnet porphyroblasts reveal a gradual, but complex, growth zonation with Mn content showing a bell-shaped pattern and Mg generally increasing towards the rim ($X_{Sps}$ 8→4; $X_{Prp}$ 8→17). Variations in $X_{Fe}$ in garnet indicate the presence of two main zones in the OS198 garnets: a garnet core with $X_{Fe} \approx 89$, and garnet rim with $X_{Fe} \approx 85$. The garnet core is characterized by a Ca increase ($X_{Grs}$ 9→12) that is concomitantly balanced by a decrease in Fe ($X_{Alm}$ 74→72). The boundary between the garnet core and rim is marked by a Ca decrease and an Fe increase ($X_{Grs} = 7$; $X_{Alm} = 75$) followed by a Ca increase and an Fe decrease ($X_{Grs} = 9$; $X_{Alm} = 73$) towards the garnet edge. Staurolite is homogeneous with $X_{Fe} = 87$–88. Biotite inclusions in the outer part of the garnet rim have $X_{Fe} = 45$. Matrix biotites defining the S2 foliation show significantly higher Fe content ($X_{Fe} = 54$) than the biotite inclusions. Tabular plagioclases that are included in garnet cores have the same Ca content as the generally homogeneous lens-shaped plagioclase grains that define the S2 foliation ($X_{Ca} = 26$). Nevertheless, some tabular plagioclases analysed within garnet rims

https://doi.org/10.1017/S0016756812000040 Published online by Cambridge University Press

Table 2. Representative analyses of minerals in the Staré Město Belt middle unit sample B26 and lower unit sample OS198

| | B26 | | | | | OS198 | | | | | | | | | |
|---|---|---|---|---|---|---|---|---|---|---|---|---|---|---|---|
| Sample | | | | | | | | | | | | | | | |
| Mineral | Grt | Grt | Bt | Bt | Ms | Grt | Grt | Bt | Bt | Ms | Chl | Chl | | Pl | Pl | Pl |
| Position | core | rim | inclusion in Grt | matrix | matrix | core zone A | rim zone C | inclusion in Grt rim | matrix | matrix | inclusion in Grt core | matrix | | inclusion in Grt core | inclusion in Grt rim | matrix |
| Wt % oxide | | | | | | | | | | | | | | | | |
| $SiO_2$ | 36.40 | 35.91 | 36.78 | 34.73 | 46.38 | 37.31 | 37.09 | 36.14 | 34.91 | 44.72 | 23.95 | 24.83 | | 61.83 | 61.34 | 62.07 |
| $TiO_2$ | 0.01 | 0.00 | 2.92 | 3.15 | 0.75 | 0.02 | 0.11 | 1.57 | 1.83 | 1.20 | 0.07 | 0.11 | | n.a. | n.a. | n.a. |
| $Cr_2O_3$ | 0.03 | 0.09 | 0.00 | 0.04 | 0.00 | 0.02 | 0.00 | 0.00 | 0.04 | 0.00 | 0.00 | 0.18 | | n.a. | n.a. | n.a. |
| $Al_2O_3$ | 19.85 | 20.60 | 20.11 | 18.83 | 36.02 | 20.94 | 21.76 | 19.52 | 19.53 | 34.92 | 21.75 | 21.63 | | 24.27 | 24.22 | 24.14 |
| $Fe_2O_3$ | n.a | n.a | n.a. | n.a. | n.a. | 0.43 | 0.37 | n.a. | n.a. | n.a. | n.a | n.a. | | n.a. | n.a. | n.a. |
| FeO | 34.74 | 34.68 | 16.72 | 22.48 | 1.78 | 33.31 | 32.43 | 16.17 | 20.43 | 1.44 | 29.73 | 25.77 | | 0.40 | 0.32 | 0.17 |
| MnO | 3.89 | 4.16 | 0.22 | 0.17 | 0.01 | 3.66 | 1.90 | 0.07 | 0.19 | 0.00 | 0.23 | 0.20 | | n.a. | n.a. | n.a. |
| MgO | 2.60 | 2.39 | 10.68 | 7.80 | 0.66 | 2.58 | 3.42 | 11.05 | 9.83 | 0.70 | 11.64 | 13.07 | | 0.00 | 0.00 | 0.00 |
| CaO | 1.86 | 1.59 | 0.00 | 0.00 | 0.00 | 2.81 | 3.03 | 0.24 | 0.00 | 0.14 | 0.01 | 0.11 | | 5.56 | 4.80 | 5.55 |
| $Na_2O$ | 0.00 | 0.00 | 0.35 | 0.14 | 0.82 | 0.00 | 0.00 | 0.00 | 0.12 | 1.33 | 0.00 | 0.00 | | 8.62 | 8.88 | 8.52 |
| $K_2O$ | 0.00 | 0.01 | 9.50 | 9.46 | 10.37 | 0.00 | 0.00 | 9.46 | 9.38 | 9.29 | 0.00 | 0.09 | | 0.17 | 0.07 | 0.08 |
| Total | 99.38 | 99.42 | 97.28 | 96.80 | 96.79 | 101.08 | 100.11 | 94.22 | 96.26 | 93.74 | 87.38 | 86.01 | | 100.85 | 99.63 | 100.53 |
| No. of O | 12 | 12 | 22 | 22 | 22 | 12 | 12 | 22 | 22 | 22 | 28 | 28 | | 8 | 8 | 8 |
| Si | 2.988 | 2.949 | 5.395 | 5.296 | 6.093 | 2.985 | 2.961 | 5.465 | 5.291 | 6.050 | 5.203 | 5.362 | | 2.728 | 2.733 | 2.740 |
| Ti | 0.001 | 0.000 | 0.322 | 0.361 | 0.074 | 0.001 | 0.007 | 0.179 | 0.209 | 0.122 | 0.011 | 0.018 | | – | – | – |
| Cr | 0.002 | 0.006 | 0.000 | 0.005 | 0.000 | 0.001 | 0.000 | 0.000 | 0.005 | 0.000 | 0.000 | 0.031 | | – | – | – |
| Al | 1.921 | 1.994 | 3.476 | 3.385 | 5.577 | 1.975 | 2.048 | 3.479 | 3.490 | 5.570 | 5.571 | 5.505 | | 1.262 | 1.272 | 1.256 |
| $Fe^{3+}$ | – | – | – | – | – | 0.026 | 0.022 | – | – | – | – | – | | – | – | – |
| $Fe^{2+}$ | 2.385 | 2.381 | 2.051 | 2.867 | 0.196 | 2.229 | 2.165 | 2.045 | 2.590 | 0.163 | 5.402 | 4.654 | | 0.015 | 0.012 | 0.006 |
| Mn | 0.271 | 0.289 | 0.027 | 0.022 | 0.001 | 0.248 | 0.128 | 0.009 | 0.024 | 0.000 | 0.042 | 0.037 | | – | – | – |
| Mg | 0.318 | 0.292 | 2.335 | 1.772 | 0.129 | 0.308 | 0.407 | 2.491 | 2.220 | 0.141 | 3.769 | 4.207 | | 0.000 | 0.000 | 0.000 |
| Ca | 0.164 | 0.140 | 0.000 | 0.000 | 0.000 | 0.241 | 0.259 | 0.039 | 0.000 | 0.020 | 0.002 | 0.026 | | 0.263 | 0.229 | 0.263 |
| Na | 0.000 | 0.000 | 0.100 | 0.041 | 0.209 | 0.000 | 0.000 | 0.000 | 0.035 | 0.349 | 0.000 | 0.000 | | 0.737 | 0.767 | 0.729 |
| K | 0.000 | 0.001 | 1.778 | 1.840 | 1.738 | 0.000 | 0.000 | 1.825 | 1.814 | 1.604 | 0.000 | 0.026 | | 0.010 | 0.004 | 0.005 |
| Total | 8.050 | 8.052 | 15.484 | 15.589 | 14.017 | 8.013 | 7.997 | 15.530 | 15.678 | 14.019 | 20.000 | 19.866 | | 5.015 | 5.017 | 4.999 |
| $X_{Fe}$ | 88.2 | 89.0 | 46.8 | 61.8 | 60.2 | 87.9 | 84.1 | 45.1 | 53.8 | 53.5 | 58.9 | 52.5 | $X_{Ca}$ | 26.0 | 23.0 | 26.3 |
| $X_{alm}$ | 76.0 | 76.7 | | | | 73.7 | 73.2 | | | | | | | | | |
| $X_{sps}$ | 8.6 | 9.3 | | | | 8.2 | 4.3 | | | | | | | | | |
| $X_{prp}$ | 10.1 | 9.4 | | | | 10.1 | 13.7 | | | | | | | | | |
| $X_{grs}$ | 5.2 | 4.5 | | | | 8.0 | 8.7 | | | | | | | | | |

n.a. – not analysed.

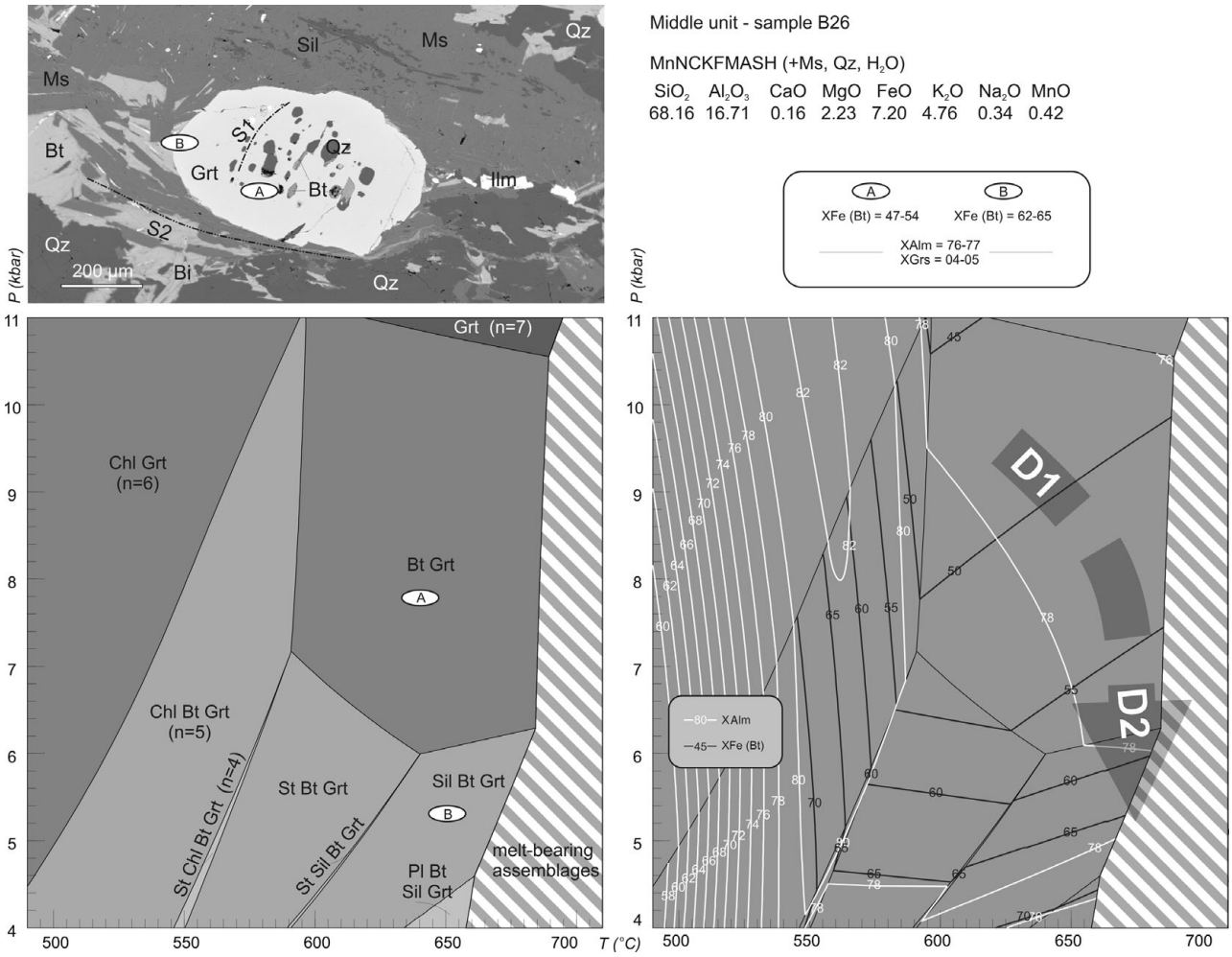


Figure 9. Mineral chemistry and thermobarometry for sample B26 from the middle unit. The dashed grey arrow refers to *P–T* evolution deduced from variations in mineral parageneses and in biotite composition.

reveal a slightly lower Ca content ($X_{Ca} = 23$). Chlorite inclusions in garnet have $X_{Fe} = 59$, whereas matrix chlorite has $X_{Fe} = 53$ (Table 2).

### *4.d.3. Pseudosection and isopleth modelling*

The phases considered in the calculation were garnet, biotite, muscovite, chlorite, staurolite, plagioclase, kyanite, sillimanite, andalusite, liquid, quartz and water. Water was assumed to be in excess for subsolidus conditions. The modelled MnNCKFMASH pseudosection indicated a stability field of plagioclase wider than that calculated for samples of the upper and lower units (Fig. 10). This is in accord with the significant amount of plagioclase in this sample and its occurrence both in the matrix and garnet cores. The prograde mineral assemblage was stable during the growth of the garnet cores and is represented by the four-variant field Grt–Pl–St–Chl–Ms–Qz. A stability field of this paragenesis is located in the temperature range of 500–600 °C and in the pressure range of 3–8 kbar. Staurolite $X_{Fe}$ values indicate that this mineral formed at approximately the same pressure conditions as the garnet cores. Contouring the mineral compositional isopleths of the garnet cores gives temperature and pressure increases from ~ 580 to ~ 600 °C and from ~ 6.2 to ~ 7.8 kbar. The presence of kyanite in sample OS198 implies that the *P–T* path must have reached the four-variant field Pl–Grt–St–Ky–Ms–Qz. The compositions of the garnet rim and the plagioclase ($X_{Ca} = 23$) included in the garnet rim indicate *P–T* conditions of 650 °C and ~ 7.5 kbar, which is enough to allow kyanite to crystallize. Changes in plagioclase $X_{Ca}$ and biotite $X_{Fe}$ from biotite inclusions in the outer garnet rims relative to analogous matrix plagioclase and biotite compositions (Fig. 10) indicate that pressure and temperature decreased. This concurs with changes in garnet composition and suggests a continuous *P–T* path transition from the four-variant field Pl–Grt–St–Ky–Ms–Qz to the four-variant field Pl–Grt–St–Bt–Ms–Qz and a change in *P–T* conditions from 650 °C and 7.5 kbar to ~ 600 °C and 6 kbar. In addition, matrix chlorite composition ($X_{Fe} = 53$) indicates that the D3-related reactivation of the S2 planes were connected with continuous retrogression and with a temperature decrease to below 570 °C.

https://doi.org/10.1017/S0016756812000040 Published online by Cambridge University Press

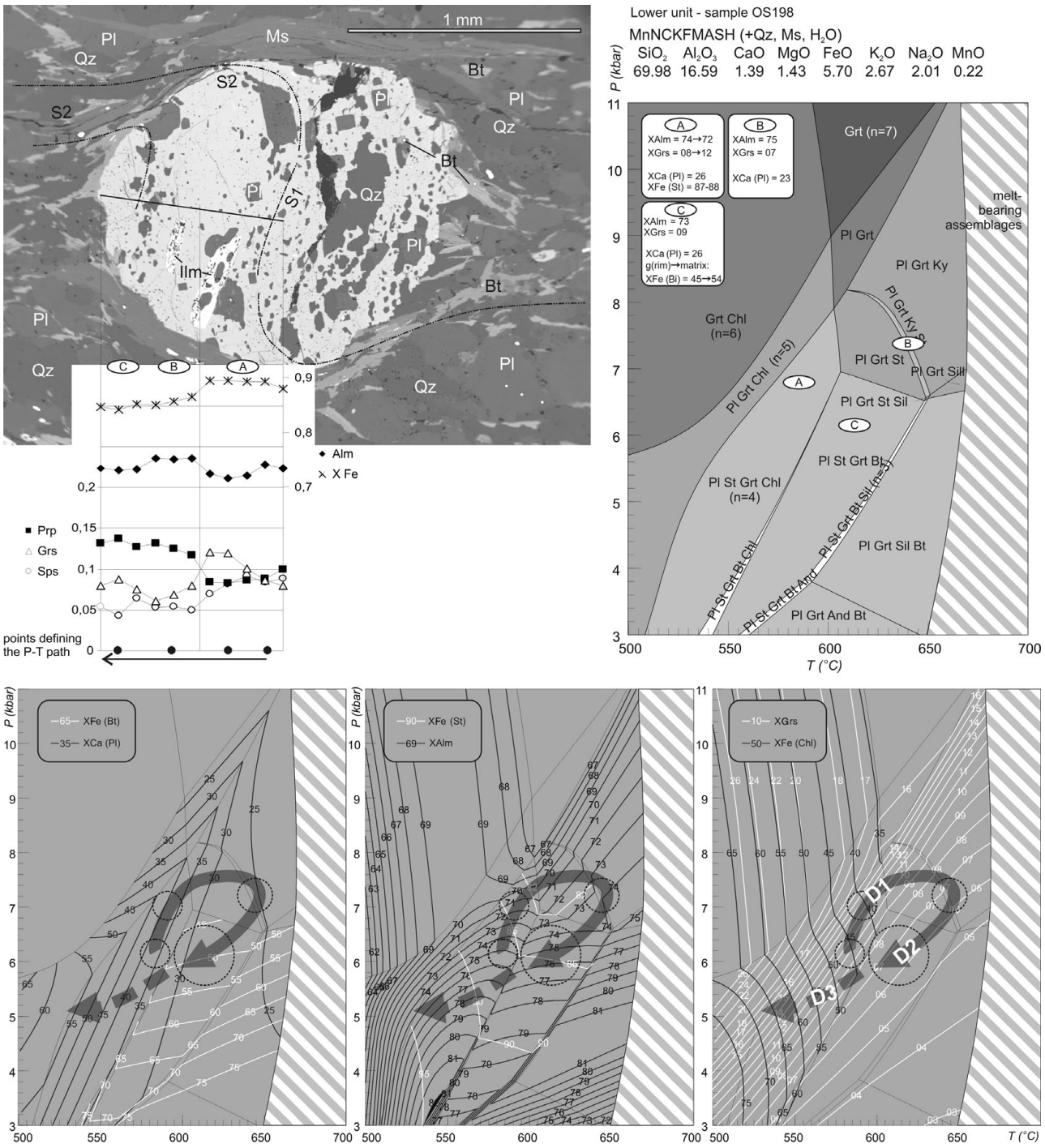


Figure 10. Mineral chemistry and thermobarometry for sample OS198 from the lower unit. Lower diagrams show selected compositional isopleths for garnet, plagioclase, staurolite, biotite and chlorite. Dashed-line circles and grey arrows indicate the *P–T* paths derived from the compositional isopleths.

## 5. Discussion

### 5.a. Correlation of three *P–T*–deformational evolutions in the frame of the Staré Město Belt

Although the pseudosection analyses performed on the metasedimentary rocks provide insight into the limited *P–T* histories of the upper, middle and lower units of the Staré Město Belt, differences in their *P–T* record are evident. Pseudosection and isopleth thermobarometry from all studied samples reveals that the transition conditions from S1 to S2 foliation planes changed along a decompression path (Fig. 11). The S1 foliation developed at depths corresponding to the following limits: 6.5 kbar at $> 570\,^{\circ}C$ in the upper unit, 9 kbar at $\sim 680\,^{\circ}C$ in the middle unit and 7.5 kbar at $\sim 650\,^{\circ}C$ in the lower unit. Thermobarometry applied to the studied metapelitic intercalation in the amphibolite body of the middle unit concurs with granulite-facies conditions deduced in previous studies from mica schists and surrounding amphibolites (Parry

https://doi.org/10.1017/S0016756812000040 Published online by Cambridge University Press

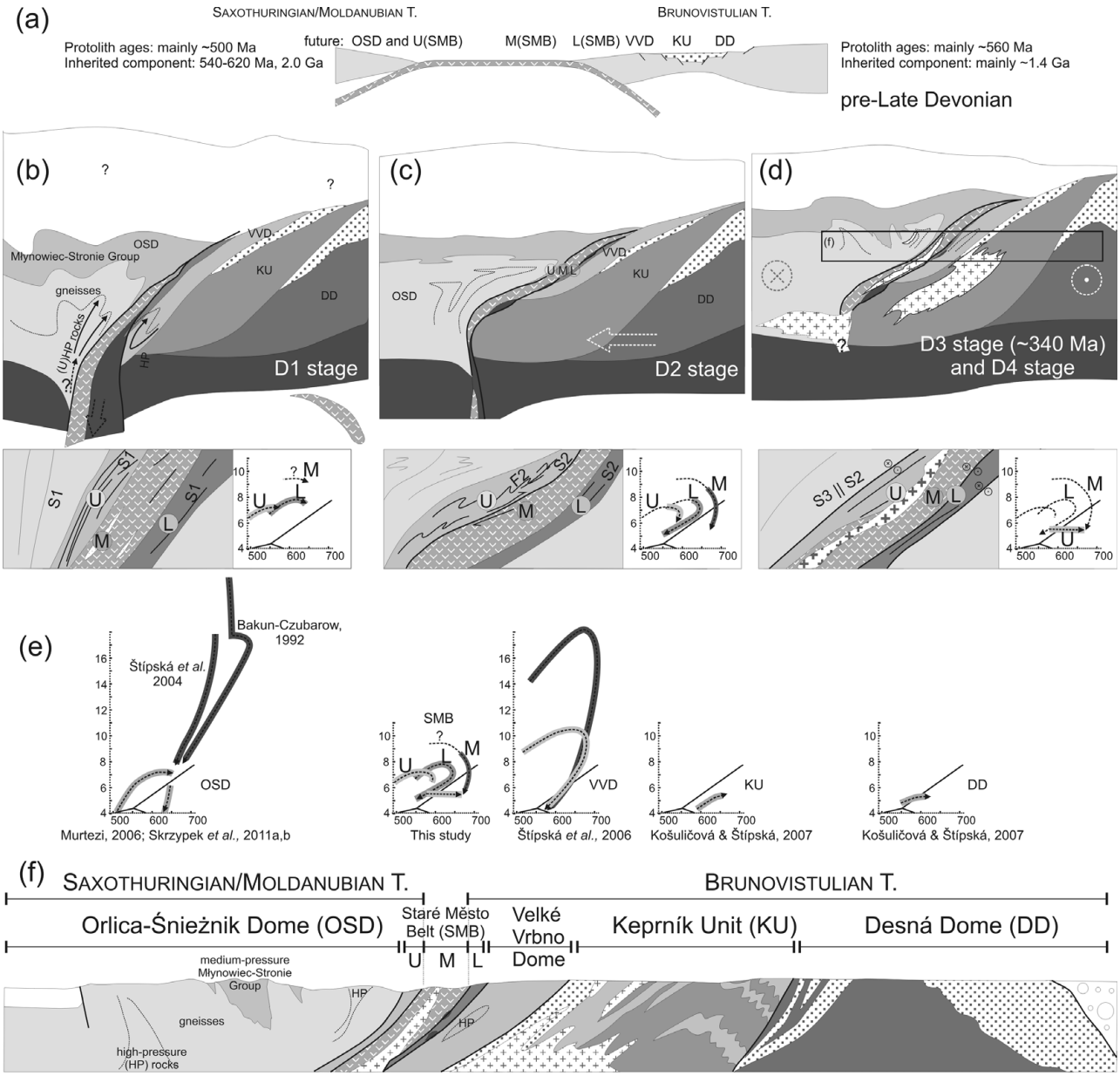


Figure 11. Tentative scenario for a polyphase tectonic evolution of the Staré Město Belt with respect to the *P–T* records of the Orlica–Śnieżnik Dome and the Silesian Domain. (a) Pre-Late Devonian separation of the two continental domains. Subduction directions are according to Kalvoda *et al*. (2008). (b) D1: the E–W-directed, Variscan collision of the Saxothuringian and Brunovistulian terranes. (c) D2: the continuous underthrusting of the Brunovistulian terrane. (d) D3: *c*. 340 Ma dextral strike-slip movements in the WNW-dipping suture zone locally associated with nearly isobaric heating related to the emplacement of the Carboniferous tonalite body. D4: the continued E–W-directed shortening. (e) Summary of the selected *P–T* data for the respective units. (f) The simplified cross-section (~ 60 km long) through the study area (the figure legend refers to Fig. 1). Letters 'U', 'M' and 'L' inscribed in circles represent the position of the upper, middle and lower unit rock samples used in this study.

*et al*. 1997; Bartz, 2004; Lexa *et al*. 2005). However, owing to the relationships between the S1 inclusion trails and the matrix S2 foliation, as well as the evidence from other regional metapelites that are thought to have resulted from Variscan tectonometamorphism (Mazur, Aleksandrowski & Szczepański, 2005; Murtezi, 2006; Štípská, Pitra & Powell, 2006; Košuličová & Štípská, 2007; Jastrzębski, 2009; Skrzypek *et al*. 2011*a*), the middle unit is considered here to represent the lowermost part of the Variscan, and not a Cambro-Ordovician, Barrovian metamorphic sequence. The differences in *P–T* histories of the upper, middle and lower units can be explained by their different position within the collisional zone during the advancement of Variscan thrusting and/or late transpression (D3 stage) along the boundaries of the lithotectonic units.

The meso-and microscale structural data indicate that the maximum burial stage was closely followed by formation of the ESE(E)-vergent tight F2 folds and the axial planar S2 schistosity during uplift. Parry *et al*. (1997) and Schulmann & Gayer (2000) argued that the Variscan structural development of the Staré Město Belt was dominated by Carboniferous dextral transpression. Nevertheless, because of the persistently meridional

https://doi.org/10.1017/S0016756812000040 Published online by Cambridge University Press

and subhorizontal orientation of the F2 fold axes, it is unlikely that the formation of the F2 folds in the upper unit was associated with strike-slip movements, unless they are X-folds (not observed to date). The simpler interpretation of these features is that the F2 folds developed as a result of top-to-the-ESE(E) thrusting (in present-day coordinates) during a protracted direct collision. The mesoscale kinematic indicators showing top-to-the-ESE(E) transport agree with those of the ductile shear zone that developed at the bottom of the upper unit (Fig. 3). This boundary is occasionally defined by a mylonite zone a few metres thick that contains completely rounded porphyroclasts of garnet, σ-porphyroclasts of amphibole, plagioclase, kyanite and staurolite, all set in a matrix of biotite, quartz and plagioclase (Fig. 6f). The strong mylonitic fabric and the unusual composition of this rock suggest that its origin is from a mixture of the original mica schists and of the amphibolites that developed during the thrust fault formation (Fig 11c). As the underlying middle unit played the role of a rigid block during the Variscan orogeny (Štípská *et al*. 2001; Štípská, Schulmann & Kröner, 2004), the rheological differences between the middle unit and the overlying upper unit could be responsible for strain accumulation along this boundary during the top-to-ESE thrusting. In conclusion, it is proposed that the syn-metamorphic tectonic burial (D1) and the uplift events (D2) distinguished in the Staré Město Belt resulted from a tectonic shortening in an ESE–WNW direction, the latter with top-to-the-E shear component.

The structural and the pseudosection analyses indicate that the dextral (top-to-the-NNE) shearing of the D3 stage was superimposed on the D2 fabric. Progressive cooling of the ∼340 Ma old tonalite intrusion in the axial part of the Staré Město Belt was syn-tectonic with the subhorizontal, dextral movements (e.g. Parry *et al*. 1997) attributed to the D3 tectonic stage in the adjacent metamorphic rocks. The L3 mineral lineation has a dextral (top-to-the-NNE) shear sense and a similar orientation to the lineations as defined by plagioclase and amphibole crystals (Fig. 2), as well as the magnetic lineation measured in the tonalite sill (Parry *et al*. 1997). Moreover, the isopleth thermobarometry applied to the Grt–Bt–Ms–Sil–Qz paragenesis in the upper unit indicates that top-to-the-NNE shearing was locally associated with nearly isobaric heating, from 600 to 650 °C, which could be an effect of the tonalite intrusion (Fig. 8). All these features indicate that the top-to-the-NNE (dextral) movements and reactivation of the S2 planes were coeval with the emplacement of the tonalite sill. Many of the observed shear zones with top-to-the-NNE shear sense, however, developed under retrogressive conditions, e.g. sample OS198 (Fig. 10). Different temperature conditions during the dextral shearing can be explained in two ways. First, the studied domains were located at different distances from the tonalite intrusion; second, the development of the dextral shear zones in this area was a long-lasting process that took place under retrogressive amphibolite- to greenschist-facies metamorphism. The second interpretation is supported by Parry *et al*. (1997) who distinguished two generations of shear zones, both with a top-to-the-NE shear sense.

*P–T* conditions of the progressive regional metamorphism of the middle and lower unit (Figs 9, 10) and the contact metamorphism of the upper unit both yielded temperatures close to the onset of melt-bearing assemblages (Fig. 8). The leucosome patches and veins are often observed in outcrops of the middle unit, i.e. adjacent to those of the tonalite body. This suggests that the partial migmatization of the metamorphic rocks was coeval with the syn-D3 emplacement of the tonalites, so producing heating to temperatures that could induce partial melting. However, the structural observations indicate that the leucosome patches already existed before the D3 shearing. It is, thus, more probable that most of localized partial melting processes and the development of granitic segregations were coeval with the temperature peak of regional metamorphism produced at the termination of the D2 tectonic stage.

The three lithostratigraphic units of the Staré Město Belt are bounded by regional-scale faults (Don, Skácel & Gotowała, 2003). As presented above, the boundary between the upper and middle zone of the Staré Město Belt shows evidence for mylonitic deformation related to top-to-the-ESE thrusting. The other boundaries of the three units are marked by an increasing concentration of dextral (top-to-the-NNE) shear zones in adjacent outcrops that suggest the same kinematics of movement along these dislocations. These observations suggest that the Bialskie, West and East Nýznerov thrusts are polyphase fractures operating during the same tectonic development that is recognized in the metasedimentary rocks (Fig. 11c, d).

### 5.b. Position and geodynamic significance of the upper, middle and lower units

Owing to lithological and geochemical similarities, rocks of the upper unit ('Hranična Formation') are traditionally considered to be equivalent to rocks of the Stronie Formation in the Orlica–Śnieżnik Dome (Don, Skácel & Gotowała, 2003; Murtezi, 2006). Hence, together with the Orlica–Śnieżnik Dome (Jastrzębski *et al*. 2010), the upper unit possibly represents one of the most peripheral units related to the Bohemian Massif terranes.

The crucial issue for the tectonic reconstruction of the Staré Město Belt is to determine the significance of the MORB-like amphibolites that are sandwiched between the metasedimentary upper and lower units. These rocks are considered to be lithospheric remnants of either an Early Palaeozoic protorift (Floyd *et al*. 1996; Kröner *et al*. 2000) or, possibly, a Rheic ocean that separated the Armorican Terrane Assemblage and the Brunovistulian terrane during Early Palaeozoic time (e.g. Aleksandrowski & Mazur, 2002; Kalvoda *et al*.

https://doi.org/10.1017/S0016756812000040 Published online by Cambridge University Press

2008). The hinterland and foreland units i.e. the Orlica–Śnieżnik Dome and the Silesian Domain have different, respectively, Early Palaeozoic and Neoproterozoic protolith ages (e.g. Kröner *et al*. 2000). Moreover, recent zircon studies have revealed the presence of 1.4 Ga inherited zircons in rocks of the Silesian Zone (e.g. Oberc-Dziedzic *et al*. 2003; Żelaźniewicz *et al*. 2005; Klimas, Kryzar & Fanning, 2009; Mazur *et al*. 2010) and lack of such zircons in rocks of the hanging wall of the collisional structure (e.g. Jastrzębski *et al*. 2010). The latter feature is widely used to discriminate Avalonian from Armorican terranes within the Variscan belt (e.g. Friedl *et al*. 2000; Zeh *et al*. 2001). These observations would speak in favour of the second option and suggest that the Staré Město MORB-like amphibolites may represent the non-subducted part of the oceanic crust extended between the two terranes (Fig. 11a), as was proposed for the Rehberg and Letovice ophiolites in the Moravian part of the Moldanubian Thrust Zone (e.g. Höck, Montag & Leichmann, 1997).

Slices of deep-seated rocks (serpentinites and possibly eclogites) included along the West and East Nýznerov thrusts and sporadically observed within the metasedimentary rocks of the lower unit (Fig. 3) indicate that this unit of the Staré Město Belt may hide remnants of a subduction zone developed between the two terranes. This view is in accordance with arguments of Štípská, Pitra & Powell (2006) emphasizing the 'Micaschists Zone' (related to the Velké Vrbno Dome and the lower unit of the Staré Město Belt in this study) as the uppermost segment of the Brunovistulian terrane. In contrast to the eclogite boudins, the metasedimentary rocks of the uppermost Brunovistulian did not experience a high-pressure episode (Štípská, Pitra & Powell, 2006; this study). Therefore, the lower unit might represent the tectonic melange of the deep-seated and medium-grade rocks that developed along the original terrane boundary (Fig. 11b, c).

### 5.c. Constraints on the tectonothermal evolution of the boundary between the Saxothuringian/Moldanubian and Brunovistulian terranes

Owing to the prominent dextral transpressive deformation, Franke & Żelaźniewicz (2002) interpreted the Moldanubian Thrust Zone as a large-scale, late Variscan dextral shear zone. This study reveals that the dextral movements are of less importance and are subsequent to the main D1–D2-related, ESE–WNW-directed collision. The regional metamorphism preceded the development of the dextral shear zone that was itself syn-tectonically intruded by the tonalite sill. This type of sill is characteristic of other late Variscan shear zones in the NE part of the Bohemian Massif (e.g. Franke & Żelaźniewicz, 2000; Aleksandrowski & Mazur, 2002).

The calculated peak pressures from samples of the three Staré Město units agree with those obtained from the metasedimentary rocks of the Svratka and Polička Crystalline Complexes (Tajčmanová *et al*. 2010) and from the metapelites of the Drossendorf unit in the eastern margin of the Moldanubian terrane (Racek *et al*. 2006). This level of consistency in pressure estimates across several geological regions indicates that the metasedimentary rocks involved in the Variscan suture zone were not buried deeper than ~ 30 km and heated to ~ 650 °C. Of greater importance is that these *P–T* conditions are also comparable with those obtained for metasedimentary rocks in adjacent areas to the Staré Město Belt, i.e. in the Orlica–Śnieżnik Dome (Murtezi, 2006; Jastrzębski, 2009; Szczepański, 2010; Skrzypek *et al*. 2011*a,b*) and in the Velké Vrbno Dome (Štípská, Pitra & Powell, 2006) (Fig. 11e). The tectonic burial of the medium-pressure rocks coeval with the exhumation of the high-pressure rocks of the Orlica–Śnieznik Dome could be an effect of a crustal-scale folding (Štípská, Schulmann & Kröner, 2004; Jastrzębski, 2009; Skrzypek *et al*. 2011*b*) that presumably resulted from the Variscan collision (Fig. 11b). Evidence for a pre-Variscan heating event, not recorded in the areas just mentioned, was recognized in rocks from the Keprník and Desna units and interpreted to indicate the pre-collisional Devonian extension of Neoproterozoic crust (Schulmann *et al*. 2005; Košuličová & Štípská, 2007) (Fig. 11a, e).

The driving force for the uplift that is recorded by the garnets in the Staré Město metasediments could be slab break-off after the initial continental collision and/or gravitational collapse of the overthickened crust. Such an instability could be responsible for the uplift and the formation of the main metamorphic foliation in both the gneisses and the metapelites of the Orlica–Śnieżnik Dome (e.g. Dumicz, 1979; Jastrzębski, 2009). Alternatively, the exhumation and development of the metamorphic S2 fabric in the Staré Město Belt could be related to the continuous indentation and underthrusting of the Brunovistulian terrane as recently proposed for the Orlica–Śnieżnik Dome (Skrzypek *et al*. 2011*b*). This latter view is more consistent with the structural observations from the Staré Město Belt, which show constant top-to-the-E kinematics during formation of the D2-related metamorphic fabrics (Fig. 11c).

The concept of tectonic burial and uplift both being connected with the ESE–WNW-directed Variscan continental collision agrees with the structural studies performed in the Silesian Zone by Żelaźniewicz *et al*. (2005). These authors interpreted the W-vergent and younger E-vergent structures as being connected with subduction and an inversion and reverse shearing, respectively, both resulting from the progressive collision between the Brunovistulian terrane and the Bohemian Massif terranes (Fig. 11b, c). The proposed tectonic evolution of the northern sector of the Moldanubian Thrust Zone has many similarities with a geodynamic model of the Bohemian Massif (Schulmann *et al*. 2005). This model shows that tectonic burial in the Moldanubian terrane and

https://doi.org/10.1017/S0016756812000040 Published online by Cambridge University Press

indentation of the Brunovistulian terrane was followed by late Variscan dextral transpressive deformation, itself linked with the ~330–325 Ma magmatism and NNE-thrusting of the Moldanubian terrane over the Brunovistulian terrane.

### 5.d. The possibility of Cambro-Ordovician tectonometamorphism in the Staré Město Belt

The leptyno-amphibolites of the middle unit have been considered to preserve a Cambro-Ordovician metamorphic fabric, which, in contrast to the WNW-dipping Variscan one, dips towards the N(NE) at shallow angles (Parry *et al*. 1997; Štípská *et al*. 2001; Štípská, Schulmann & Kröner, 2004; Lexa *et al*. 2005). However, the localized rotation of the WNW-dipping metamorphic fabrics of these rocks might be explained by late folding and/or block tectonics. Geological cross-sections, incorporating new data by the author, indicate that metamorphic fabrics in the metasediments and magmatic fabrics in the tonalities were both rotated together with the lithological contacts near the NNE-dipping fault surfaces. Distribution of rocks with WNW–ESE-striking foliations (maximum B in Fig. 2) near fault surfaces of the same strike suggests that the Variscan fabrics in this area were rotated due to faulting. A late rotation of the tectonic structures is also seen from a general change in the plunge direction of meridionally trending lineations from NNE(N, NE) in the north to SSW(S, SW) in the south of the Orlica–Śnieżnik Dome and Staré Město Belt (Kasza, 1964; Don, Skácel & Gotowała, 2003; this study). Locally, the foliation dips to the ESE (maximum C in Fig. 2), and this suggests a rotation of the S2‖S3 foliation around the N–S-trending F4 folds. As a consequence, the different orientations of the Staré Město Belt metamorphic foliations cannot be used as diagnostic criteria to discriminate between Cambro-Ordovician and Variscan fabrics. The high-temperature Cambro-Ordovician deformation was mainly deduced from the presence of ~500 Ma old zircons in melt patches that cross-cut the main metamorphic fabric in the amphibolites (Kröner *et al*. 2000). The structural and pseudosection analyses of the adjacent metasedimentary rocks show that the granulite-facies metamorphism of the middle unit as well as the local *in situ* partial melting in the Staré Město Belt and the development of associated melt patches and veins were presumably coeval with the Variscan metamorphic event(s). Thus, no direct evidence for Cambro-Ordovician metamorphism of the Staré Město Belt was found.

## 6. Conclusions

The tectonometamorphic evolution of the Staré Město Belt resulted from Variscan continental collision, presumably coupled with the closure of the oceanic tract between Armorican Terrane Assemblage (Saxo-thuringian or Moldanubian terrane of the Bohemian Massif) and the Brunovistulian terrane. A synthesis of new and existing data indicates that the upper unit of the Staré Město Belt ('Hranična Formation') could be correlated with metavolcano-sedimentary rocks of the Orlica–Śnieżnik Dome and it occupies the easternmost hinterland position. The lower metasedimentary unit could be correlated with the Velké Vrbno Dome, thus it possibly forms the westernmost tectonic sheet of the Brunovistulian terrane. The middle unit of the Staré Město Belt, i.e. MORB-like amphibolites and associated migmatized mica schists, coincides with a Variscan boundary between the two different terranes.

The frontal ESE–WNW-directed (in present-day coordinates) Variscan continental collision led to tectonic burial of all three units of the Staré Město Belt. This burial was followed by the underthrusting of the Brunovistulian terrane that led to eastward folding and the formation of the axial planar, WNW-dipping schistosity. At the termination of this stage, the temperature peak of the regional metamorphism occurred, which led to a partial melting of the metasedimentary rocks. The three units exhibit variations in their respective temperature peak conditions, the highest of which are observed for the middle unit rocks.

These events were followed by the ~340 Ma dextral strike-slip movements along the Variscan suture zone that was syn-tectonically intruded by a tonalite sill. The boundaries between the lithotectonic units of the belt are the polyphase fractures operating during the tectonic evolution deduced from the metasediments. Localized rotation of the moderately WNW-dipping metamorphic fabrics into shallowly NE-dipping ones in the studied rocks is explained most reasonably by late folding events and/or block tectonics.

**Acknowledgements.** I wish to thank Prof. Andrzej Żelaźniewicz for guidance and comments that considerably improved the manuscript. I would like to thank two anonymous referees for constructive comments that greatly improved the presentation. I also acknowledge the kind help of Drs Ryszard Orłowski and Piotr Dzierżanowski for operating the microprobe. Patrick Roycroft is thanked for critically reading the manuscript and correcting the English. This work was supported by MNiSW grant no. N 307 112436 during the period 2009 to 2011.

## References

ALEKSANDROWSKI, P. & MAZUR, S. 2002. Collage tectonics in the northeasternmost part of the Variscan Belt: the Sudetes, Bohemian Massif. In *Palaeozoic Amalgamation of Central Europe* (eds J. A. Winchester, T. C. Pharaoh & J. Verniers), pp. 237–77. Geological Society of London, Special Publication no. 201.

BAKUN-CZUBAROW, N. 1992. Quartz pseudomorphs after coesite and quartz exsolutions in eclogitic clinopyroxenes of the Złote Mountains in the Sudetes (SW Poland). *Archiwum Mineralogiczne* **48**, 3–25.

BARTZ, W. 2004. Metamorphic evolution of the amphibolites from the polish part of Stare Město Zone (Sudetes, SW Poland). *Mineralogia Polonica* **35**, 5–74.

https://doi.org/10.1017/S0016756812000040 Published online by Cambridge University Press

CHÁB, J., MIXA, P, VANĚČEK, M. & ŽAČEK, V. 1994. Evidence of an extensional tectonics in the NW of the Hrubý Jeseník Mts. (the Bohemian massif, Central Europe). *Věstnik Českého geologického ústavu* **69**, 7–15.

COGGON, R. & HOLLAND, T. J. B. 2002. Mixing properties of phengitic micas and revised garnet-phengite thermobarometers. *Journal of Metamorphic Geology* **20**, 683–96.

DON, J. 1982. The Sienna Synform and the relationship of gneisses to the deformational stages distinguished in the Śnieżnik Metamorphic Massif (Sudetes). *Geologia Sudetica* **17**, 103–24.

DON, J., DUMICZ, M., WOJCIECHOWSKA, I. & ŻELAŹNIEWICZ, A. 1990. Lithology and tectonics of the Orlica–Śnieżnik Dome, Sudetes – Recent State of Knowledge. *Neues Jahrbuch für Geologie und Paläontologie, Abhandlungen* **197**, 159–88.

DON, J., SKÁCEL, J. & GOTOWAŁA, R. 2003. The boundary zone of the East and West Sudetes on the 1:50 000 scale geological map of the Velké Vrbno, Staré Město and Śnieżnik Metamorphic Units. *Geologia Sudetica* **35**, 25–59.

DUMICZ, M. 1979. Tectogenesis of the metamorphosed series of the Kłodzko District: a tentative explanation. *Geologia Sudetica* **14**, 29–46.

DUTCH, R. A., HAND, M. & KELSEY, D. E. 2010. Unravelling the tectonothermal evolution of reworked Archaean granulite-facies metapelites using in situ geochronology, an example from the Gawler Craton, Australia. *Journal of Metamorphic Geology* **28**, 293–316.

FINGER, F., GERDES, A., JANOUŠEK, V., RENÉ, M. & RIEGLER, G. 2007. Resolving the Variscan evolution of the Moldanubian sector of the Bohemian Massif: the significance of the Bavarian and Moravo-Moldanubian tectonometamorphic phases. *Journal of Geosciences* **52**, 9–28.

FINGER, F., HANZL, P., PIN, C., VON QUADT, A. & STEYRER, H. P. 2000.The Brunovistulian: Avalonian Precambrian at the eastern end of the Central European Variscides? In *Orogenic Processes: Quantification and Modelling in the Variscan Belt* (eds W. Franke, V. Haak, O. Oncken & D. Tanner), pp. 103–12. Geological Society of London, Special Publication no. 179.

FLOYD, P. A., WINCHESTER, J., CIESIELCZUK, J., LEWANDOWSKA, A., SZCZEPAŃSKI, J. & TURNIAK, K. 1996. Geochemistry of early Palaeozoic amphibolites from the Orlica-Śnieżnik dome, Bohemian massif: petrogenesis and palaeotectonic aspects. *Geologishe Rundschau* **85**, 225–38.

FRANKE, W. & ŻELAŹNIEWICZ, A. 2000. The eastern termination of the Variscides: terrane correlation and kinematic evolution. In *Orogenic Processes: Quantification and Modelling in the Variscan Belt* (eds W. Franke, V. Haak, O. Oncken & D. Tanner), pp. 63–86. Geological Society of London, Special Publication no. 179.

FRANKE, W. & ŻELAŹNIEWICZ, A. 2002. Structure and evolution of the Bohemian Arc. In *Palaeozoic Amalgamation of Central Europe* (eds J. A. Winchester, T. C. Pharaoh & J. Verniers), pp. 279–93. Geological Society of London, Special Publication no. 201.

FRIEDL, G., FINGER, F., MCNAUGHTON, N. J. & FLETCHER, I. R. 2000. Deducing the ancestry of terranes: SHRIMP evidence for South America-derived Gondwana fragments in central Europe. *Geology* **28**, 1035–8.

HÖCK, V., MONTAG, O. & LEICHMANN, J. 1997. Ophiolite remnants at the eastern margin of the Bohemian Massif and their bearing on the tectonic evolution. *Mineralogy and Petrology* **60**, 267–87.

HOLLAND, T. J. B., BAKER, J. M. & POWELL, R. 1998. Mixing properties and activity-composition relationships of chlorites in the system MgO-FeO-$Al_2O_3$-$SiO_2$-$H_2O$. *European Journal of Mineralogy* **10**, 395–406.

HOLLAND, T. J. B. & POWELL, R. 1998. An internally consistent thermodynamic data set for phases of petrological interest. *Journal of Metamorphic Geology* **16**, 309–43.

HOLLAND, T. J. B. & POWELL, R. 2003. Activity-composition relations for phases in petrological calculations: an asymmetric multicomponent formulation. *Contributions to Mineralogy and Petrology* **145**, 492–501.

JASTRZĘBSKI, M. 2009. A Variscan continental collision of the West Sudetes and the Brunovistulian terrane: a contribution from structural and metamorphic record of the Stronie Formation, the Orlica-Śnieżnik Dome, SW Poland. *International Journal of Earth Sciences* **98**, 1901–23.

JASTRZĘBSKI, M., ŻELAŹNIEWICZ, A., NOWAK, I., MURTEZI, M. & LARIONOV, A. N. 2010. Protolith age and provenance of metasedimentary rocks in Variscan allochthon units: U–Pb SHRIMP zircon data from the Orlica–Śnieżnik Dome, West Sudetes. *Geological Magazine* **147**, 416–33.

KALVODA, J., BÁBEK, O., FATKA, O., LEICHMANN, J., MELICHAR, R. & ŠPAČEK, P. 2008. Brunovistulian terrane (Bohemian Massif, Central Europe) from late Proterozoic to late Paleozoic: a review. *International Journal of Earth Sciences* **97**, 497–517.

KASZA, L. 1964 Budowa geologiczna górnego dorzecza Białej Lądeckiej. *Geologia Sudetica* **1**, 119–67.

KLIMAS, K., KRYZA, R. & FANNING, C. M. 2009. Palaeo- to Mesoproterozoic inheritance and Ediacaran anatexis recorded in gneisses at the NE margin of the Bohemian Massif: SHRIMP zircon data from the Nowolesie gneiss, Fore-Sudetic Block (SW Poland). *Geologia Sudetica* **41**, 25–42.

KOŠULIČOVÁ, M. & ŠTÍPSKÁ, P. 2007. Variations in the transient prograde geothermal gradient from chloritoid-staurolite equilibria: a case study from the Barrovian and Buchan-type domains in the Bohemian Massif. *Journal of Metamorphic Geology* **25**, 19–36.

KRETZ, R. 1983. Symbols for rock-forming minerals. *American Mineralogist* **68**, 277–9.

KRÖNER, A., ŠTÍPSKÁ, P., SCHULMANN, K. & JAECKEL, P. 2000. Chronological constraints on the pre-Variscan evolution of the northeastern margin of the Bohemian Massif, Czech Republic. In *Orogenic Processes: Quantification and Modelling in the Variscan Belt* (eds W. Franke, V. Haak, O. Oncken & D. Tanner), pp. 175–97. Geological Society of London, Special Publication no. 179.

LEXA, O., ŠTÍPSKÁ, P., SCHULMANN, K., BARATOUX, L. & KRÖNER, A. 2005. Contrasting textural record of two distinct metamorphic events of similar P-T conditions and different durations. *Journal of Metamorphic Geology* **23**, 649–66.

LINNEMANN, U., PEREIRA, F., JEFFRIES, T. E., DROST, K. & GERDES, A. 2008. The Cadomian Orogeny and the opening of the Rheic Ocean: the diachrony of geotectonic processes constrained by LA-ICP-MS U–Pb zircon dating (Ossa-Morena and Saxo-Thuringian Zones, Iberian and Bohemian Massifs). *Tectonophysics* **461**, 21–43.

MAHAR, E. M., BAKER, J. M., POWELL, R., HOLLAND, T. J. B. & HOWELL, N. 1997. The effect of Mn on mineral stability in metapelites. *Journal of Metamorphic Geology* **15**, 223–38.

MAZUR, S., ALEKSANDROWSKI, P., SZCZEPAŃSKI, J. 2005. The presumed Tepla-Barrandian / Moldanubian terrane boundary in the Orlica Mountains (Sudetes, Bohemian Massif): structural and petrological characteristics. *Lithos* **82**, 85–112.

MAZUR, S., KRÖNER, A., SZCZEPAŃSKI, J., TURNIAK, K., HANZL, P., MELICHAR, R., RODIONOV, N. V., PADERIN, I. & SERGGEV, S. A. 2010. Single zircon U–Pb ages and geochemistry of granitoid gneisses from SW Poland: evidence for an Avalonian affinity of the Brunian microcontinent. *Geological Magazine* **147**, 508–26.

MURTEZI, M. 2006. The acid metavolcanic rocks of the Orlica–Śnieżnik Dome: their origin and tectono-metamorphic evolution. *Geologia Sudetica* **38**, 1–38.

OBERC-DZIEDZIC, T., KLIMAS, K., KRYZA, R. & FANNING, C. M. 2003. SHRIMP zircon geochronology of the Strzelin gneiss, SW Poland: evidence for a Neoproterozoic thermal event in the Fore-Sudetic Block, Central European Variscides. *International Journal of Earth Sciences* **92**, 701–11.

OPLETAL, M., JELINEK, E., PEČINA, V., POŠMOURTNÝ, K. & POUBOVÁ, E. 1990. Metavolcanites of the SE part of the Lugicum, their geochemistry and geotectonic interpretation. *Sbornik Geologickych Ved, Geologie* **45**, 37–64.

PARRY, M., ŠTÍPSKÁ, P., SCHULMANN, K., HROUDA, F., JEŽEK, J. & KRÖNER, A. 1997. Tonalite sill emplacement at an oblique boundary: northeastern margin of the Bohemian Massif. *Tectonophysics* **280**, 61–81.

POUBOVÁ, E. & SOKOL, A. 1992. The petrology and geochemistry of the metaophiolitic rocks of Stare Mesto crystalline unit. *Krystalinikum* **21**, 67–88.

RACEK, M., ŠTÍPSKÁ, P., PITRA, P., SCHULMANN, K. & LEXA, O. 2006. Metamorphic record of burial and exhumation of orogenic lower and middle crust: a new tectonothermal model for the Drosendorf window (Bohemian Massif, Austria). *Mineralogy and Petrology* **86**, 221–51.

SAWICKI, L. 1995. *Geological Map of Lower Silesia with adjacent Czech and German Territories 1:100 000*. Warszawa: Państwowy Instytut Geologiczny.

SCHULMANN, K. & GAYER, R. 2000. A model of an obliquely developed continental accretionary wedge: NE Bohemian Massif. *Journal of the Geological Society, London* **156**, 401–16.

SCHULMANN, K., KRÖNER, A., HEGNER, E., WENDT, I., KONOPÁSEK, J., LEXA, O. & ŠTÍPSKÁ, P. 2005. Chronological constraints on the pre-orogenic history, burial and exhumation of deep-seated rocks along the eastern margin of the Variscan orogen, Bohemian Massif, Czech Republic. *American Journal of Science* **305**, 407–48.

SIIVOLA, J. & SCHMID, R. 2007. *List of Mineral Abbreviations: Recommendations by the IUGS Subcommission on the Systematics of Metamorphic Rocks*. Web version 01–02-07. IUGS Commission on the Systematics in Petrology.

SKÁCEL, J. 1989. Hranice lugika a silezika (středních a východních Sudet). *Prace Geologiczno-Mineralogiczne – Acta Universitatis Wratislaviensis* **17**, 45–55.

SKRZYPEK, E., SCHULMANN, K., ŠTÍPSKÁ, P., CHOPIN, F., LEHMANN, J., LEXA, O. & HALODA, J. 2011*a*. Tectono-metamorphic history recorded in garnet porphyroblasts: insights from thermodynamic modelling and electron backscatter diffraction analysis of inclusion trails. *Journal of Metamorphic Geology* **29**, 473–96.

SKRZYPEK, E., ŠTÍPSKÁ, P., SCHULMANN, K., LEXA, O. & LEXOVA, M. 2011*b*. Prograde and retrograde metamorphic fabrics – a key for understanding burial and exhumation in orogen (Bohemian Massif). *Journal of Metamorphic Geology* **29**, 451–72.

ŠTÍPSKÁ, P., PITRA, P. & POWELL, R. 2006. Separate or shared metamorphic histories of eclogites and surrounding rocks? An example from the Bohemian Massif. *Journal of Metamorphic Geology* **24**, 219–40.

ŠTÍPSKÁ, P., SCHULMANN, K. & KRÖNER, A. 2004. Vertical extrusion and middle crust spreading of omphacite granulite: a model of syn-convergent exhumation (Bohemian Massif, Czech Republic). *Journal of Metamorphic Geology* **22**, 179–98.

ŠTÍPSKÁ, P., SCHULMANN, K., THOMPSON, A. B., JEŽEK, J. & KRÖNER, A. 2001. Thermo-mechanical role of a Cambro-Ordovician paleorift during the Variscan collision: the NE margin of the Bohemian Massif. *Tectonophysics* **332**, 239–53.

SZCZEPAŃSKI, J. 2010. Geological setting of the Bystrzyckie Mts Crystalline Massif. *Mineralogia – Special Papers* **37**, 140–44.

TAIT, J. A., BACHTADSE, V., FRANKE, W. & SOFFEL, H. C. 1997. Geodynamic evolution of the European Variscan fold belt: palaeomagnetic and geological constraints. *Geologische Rundschau* **86**, 585–98.

TAJČMANOVÁ, L., SOEJONO, I., KONOPÁSEK, J., KOŠLER, J. & KLÖTZLI, U. 2010 Structural position of high-pressure felsic to intermediate granulites from NE Moldanubian domain (Bohemian Massif). *Journal of Geological Society, London* **167**, 329–45.

TINKHAM, D. K. & GHENT, E. D. 2005. Estimating P-T conditions of garnet growth with isochemical phase-diagram sections and the problem of effective bulk-composition. *Canadian Mineralogist* **43**, 35–50.

VON RAUMER, J. F., STAMPFLI, G. M. & BUSSY, F. 2003. Gondwana-derived microcontinents – the constituents of the Variscan and Alpine collisional orogens. *Tectonophysics* **365**, 7–22.

WHITE, R. W., POMROY, N. E. & POWELL, R. 2005. An in-situ metatexite-diatexite transition in upper amphibolite facies rocks from Broken Hill, Australia. *Journal of Metamorphic Geology* **23**, 579–602.

WHITE, R. W., POWELL, R. & HOLLAND, T. J. B. 2007. Progress relating to calculation of partial melting equilibria for metapelites. *Journal of Metamorphic Geology* **25**, 511–27.

WHITNEY, D. L. & EVANS, B. W. 2010. Abbreviations for names of rock-forming minerals. *American Mineralogist* **95**, 185–7.

ZEH, A., BRÄTZ, H., MILLAR, I. L. & WILLIAMS, I. S. 2001. A combined zircon SHRIMP and Sm–Nd isotope study of high-grade paragneisses from the Mid-German Crystalline Rise: evidence for northern Gondwana and Grenvillian provenance. *Journal of the Geological Society, London* **158**, 983–94.

ŻELAŹNIEWICZ, A., BUŁA, Z., FANNING, M., SEGHEDI, A. & ŻABA, J. 2009. More evidence on Neoproterozoic terranes in Southern Poland and southeastern Romania. *Geological Quarterly* **53**, 93–124.

ŻELAŹNIEWICZ, A., NOWAK, I., BACHLIŃSKI, R., LARIONOV, A. N. & SERGEEV, S. A. 2005. Cadomian versus younger deformations in the basement of the Moravo-Silesian Variscides, East Sudetes, SW Poland: U-Pb SHRIMP and Rb-Sr age data. *Geologia Sudetica* **37**, 35–51.